

CONFIDENTIAL

Copy 6  
RM E53K06

NACA RM E53K06



# RESEARCH MEMORANDUM

ANALYTICAL STUDY OF LOSSES AT OFF-DESIGN CONDITIONS  
FOR A FIXED-GEOMETRY TURBINE

By Warner L. Stewart and David G. Evans

Lewis Flight Propulsion Laboratory  
Cleveland, Ohio

CLASSIFICATION CANCELLED

Authority NACA R 7-3176 Date 11/14/55

By 27287-12/9/53 See \_\_\_\_\_

CLASSIFIED DOCUMENT

This material contains information affecting the National Defense of the United States within the meaning of the espionage laws, Title 18, U.S.C., Secs. 793 and 794, the transmission or revelation of which in any manner to an unauthorized person is prohibited by law.

NATIONAL ADVISORY COMMITTEE  
FOR AERONAUTICS

WASHINGTON

February 4, 1954

LIBRARY COPY

FEB 9 1954

LANGLEY AERONAUTICAL LABORATORY  
LIBRARY, NACA  
LANGLEY FIELD, VIRGINIA

CONFIDENTIAL



## NATIONAL ADVISORY COMMITTEE FOR AERONAUTICS

RESEARCH MEMORANDUM

## ANALYTICAL STUDY OF LOSSES AT OFF-DESIGN CONDITIONS FOR

## A FIXED-GEOMETRY TURBINE

By Warner L. Stewart and David G. Evans


## SUMMARY

An analytical investigation was made to determine the off-design loss characteristics of a fixed-geometry turbine of which the experimental performance was known. The method used in the analysis was based on a method presented in a previous report which assumed (a) a blade effective loss parameter and (b) that the velocity normal to the rotor blade entrance angle was lost as a total-pressure loss. The method used differed from that presented in the reference report in that (a) it utilized continuity at the blade throat, a station just upstream of the trailing edge, and a station just downstream of the trailing edge to obtain the flow conditions, and (b) a constant tangential component of velocity was assumed between the stations just upstream and just downstream of the trailing edge.

Good correlation between the analytically and experimentally obtained performance was found over the entire map until limiting loading was approached. The discrepancy near limiting loading resulted from the fact that the blade effective throat areas were not equal to the measured throat areas. The large decrease in efficiency at low-speed high pressure ratios and at high-speed low pressure ratios was found in the analysis to be almost entirely due to the rotor incidence and turbine exit whirl losses. The rotor exit shock losses were found to have only a small effect on the turbine efficiency. Wide ranges of rotor mean incidence angle and relative critical velocity ratio were obtained over the range of performance and greatly affected the incidence loss. From the results of the investigation, it was concluded that for turbines designed to operate efficiently at more than one point, the design must compromise rotor incidence angle and exit whirl losses.

## INTRODUCTION

In certain turbine applications, it is necessary to design the turbine to operate at more than one condition. For example, the



conditions imposed on a turbine at take-off may be considerably different from those imposed at flight conditions, and the turbine should be designed to operate efficiently at these two points. It is of interest, therefore, to know how the turbine losses may vary over the range of desired operation in order to compromise the design such that an optimum turbine for a specific application can be obtained.

An analytical investigation was conducted at the NACA Lewis laboratory to determine the loss characteristics of a fixed-geometry turbine whose performance was known. A comparison between the analytically and experimentally obtained performance over a wide range of operating conditions could be made to evaluate the analytical results. The experimental performance of the turbine chosen is presented in reference 1.

The method of analysis used was similar to that presented in reference 2 in that the same criteria of effective viscous loss and rotor incidence loss were used. The method presented herein differs from that of reference 2 in that it does not assume that the flow follows the blade exit angle at subcritical pressure ratios nor does it assume Prandtl-Meyer deflection at supercritical pressure ratios. The method utilizes a flow chart and uses continuity at the blade throat, a station just upstream from the trailing edge, and a station downstream of the trailing edge as a basis. The method assumes no change in tangential component of velocity from just upstream of the trailing edge to just downstream of the trailing edge. The turbine to be analyzed was a mixed-flow turbine in that the mean radius decreased from the rotor inlet to the rotor outlet, and this was also considered. Four types of losses were assumed in the analysis: (1) The sum of the nozzle and rotor effective viscous losses, which include the blading viscous losses, boundary-layer secondary flow losses, and tip clearance losses, (2) rotor incidence losses, (3) rotor exit shock losses (obtained only at conditions above the rotor choking point), and (4) exit whirl loss.

The purpose of this report is to present the results of the analytical investigation of the turbine of reference 1 to indicate the extent to which the various turbine losses affect the turbine efficiency over the range of performance. The variation in rotor mean relative critical velocity ratio and incidence angle over the range of performance analyzed will also be presented to indicate the range of these variables encountered. The investigation was conducted over a speed range from 40 to 120 percent design speed and from a pressure ratio of 1.4 to that corresponding to the turbine limiting work output point.

#### METHOD OF ANALYSIS

Assumptions. - The analysis conducted in this report made the two basic assumptions used in reference 2. These assumptions are:

(1) The sum of the blade loss due to friction, secondary flow, and tip clearance can be combined into an effective viscous loss dependent on a blade loss parameter K. (All symbols are defined in appendix A.) A value of K is used in the analysis such that at design speed and design specific work output the analytically obtained efficiency equaled the experimentally obtained efficiency.

(2) The component of velocity normal to the blade inlet angle is lost as a total-pressure loss. As indicated by references 2 and 3 fairly reliable off-design performance has been obtained analytically when these two assumptions are used.

The following assumptions that differ from those in reference 2 are made:

(1) Additional stations are used in the analysis. Figure 1 presents the velocity diagrams and station designations used in the analysis. These additional stations are station 2 in the nozzle and station 5 in the rotor. It is assumed that there is no change in tangential component of velocity from station 2 to station 3 in the nozzle and from station 5 to station 6 in the rotor.

(2) At supercritical pressure ratios across a blade row, continuity is used between stations 1 and 2 in the nozzle and stations 4 and 5 in the rotor to obtain the supersonic expansion. These first two assumptions have been used in the design of several turbines and the satisfactory performance obtained has indicated that the assumptions are valid.

(3) A shock loss corresponding to the supersonic velocity at stations 2 and 5 is assumed to occur. This is probably higher than that expected experimentally. However, the high loss was assumed to determine whether shock losses have an appreciable effect on the turbine efficiency.

Charts, graphs, and tables used in calculations. - A series of charts, graphs, and tables was used to facilitate the calculations of the turbine performance. The equations used to obtain these charts, graphs, and tables are presented in appendix B.

Turbine characteristics. - The following physical characteristics of the turbine and operating conditions must be known or assumed before the analysis is started. The conditions used in the analysis of the subject turbine are given as an example:

(1) Turbine inlet total conditions

$$T_0^* = 518.4 \text{ } ^\circ\text{R}$$

$$p'_0 = 2116 \text{ lb/sq ft}$$

- (2) Turbine annulus area at stations 0, 3, and 6

$$A_{\text{ann},0} = 0.545 \text{ sq ft}$$

$$A_{\text{ann},3} = 0.575 \text{ sq ft}$$

$$A_{\text{ann},6} = 0.671 \text{ sq ft}$$

- (3) Flow area in plane perpendicular to axis of rotation at stations 2 and 5

$$A_2 = 0.549 \text{ sq ft}$$

$$A_5 = 0.635 \text{ sq ft}$$

- (4) Throat area at stations 1 and 4

$$A_1 = 0.317 \text{ sq ft}$$

$$A_4 = 0.459 \text{ sq ft}$$

- (5) Mean radius ratio at station 0

$$r_m/r_t = 0.850$$

stations 1, 2, and 3

$$r_m/r_t = 0.840$$

stations 4, 5, and 6

$$r_m/r_t = 0.805$$

- (6) Rotor mean inlet blade angle (see fig. 1)

$$\theta_{r,i} = 15.4^\circ$$

- (7) Design mean wheel speed, specific work output, and rating efficiency (efficiency based on axial component of total-pressure ratio)

$$(U/V_{cr})_3 = 0.620$$

$$(\Delta h' / \theta_{cr}) = 20.2 \text{ Btu/lb}$$

$$\eta_x = 0.87$$

3076

Performance analysis procedure. - The procedure used in the performance calculations can be summarized as follows: A value of  $K$  must first be obtained such that at design speed and specific work output the calculated rating efficiency agrees with the experimentally obtained efficiency. This was done by assuming a series of  $K$  values, calculating the specific work output and rating efficiency over a range of points that span design specific work output, and then cross-plotting to obtain the value of  $K$  that would yield design efficiency at design specific work output. For this analysis it was found that  $K = 0.400$  gave the correct rating efficiency. Once  $K$  is known, a series of working curves is constructed to facilitate the calculations. Derivation and description of these curves are presented in appendix C. The calculation of the performance map can then proceed. The subject turbine was investigated at 40, 60, 80, 100, and 120 percent design speed and pressure ratios from 1.4 up to that corresponding to the turbine limiting loading point. A sample calculation is shown in appendix D to illustrate clearly the procedure used in calculating each point from a low pressure ratio up to limiting loading for a given speed. The point selected for the sample calculation is that at which the rotor choked at 100 percent design speed. The procedure for calculating the performance parameters to construct the performance maps is also illustrated in appendix D.

Loss calculation. - In order to show the effect of the various losses on the analytically obtained turbine rating efficiency, a breakdown of the losses in terms of efficiency was obtained. A sample calculation is presented in appendix E to illustrate the procedure used in making the calculations.

## RESULTS OF ANALYSIS

### Performance Map

As discussed previously, the performance of the subject turbine was obtained analytically at 40, 60, 80, 100, and 120 percent design speeds, and at pressure ratios from 1.4 to that corresponding to the limiting loading point. Figure 2 presents the analytically obtained performance map. The equivalent specific work output is shown as a function of the weight-flow - speed parameter (product of equivalent weight flow and equivalent rpm). Lines of constant rating total-pressure ratio (based on axial component of turbine exit velocity), percent design speed, and rating efficiency are shown as parameters. For comparative purposes, the experimentally obtained performance of this turbine is shown in figure 3 (data from ref. 1). It can be seen that the two performance maps are very similar even at speeds and pressure ratios far removed from the design point. The specific work output at the turbine limiting loading point is seen to be somewhat higher analytically than that obtained experimentally. The significance of this will be discussed later.

Included on the analytically obtained performance map (fig. 2) is the rotor choking line. It can be seen that once the rotor choked, the additional specific work output up to the limiting loading point was quite limited. Thus, for standard rotors in which the flow passages converge to the exit, if the turbine is designed for the rotor to choke, it will, of necessity, be operating close to the limiting loading point because of the high Mach number level at the rotor exit. Hence, the design of a turbine of this type will be critical from a limiting loading standpoint.

#### Variation of Losses Over Performance Range Investigated

The effect of the various turbine losses assumed in the turbine analysis on the turbine efficiency was calculated for the subject turbine over the performance range investigated. Before presenting these results, a comparison of the analytically and experimentally obtained rating efficiency will be presented in order that a better evaluation of the method of analysis can be made.

Comparison with experimental results. - In figure 4 is presented the effect of the turbine losses on the calculated turbine efficiency over the speed range investigated. Efficiency is shown as a function of specific work output. The lowest curve on each part of this figure represents the variation of calculated rating efficiency with specific work output. Along with this curve are actual data points from the experimental investigation of the turbine with design ratio of nozzle to rotor throat area. Also included are data points from the same turbine but with an area ratio 3 percent less than design. A comparison between the analytically and experimentally obtained efficiency using design area ratio indicates good agreement until limiting loading is approached. The turbine with the reduced area ratio, however, is in better agreement with the calculated efficiencies even up to the limiting loading point, indicating that the effective area ratio was not equal to the measured area ratio. This could be caused by a large boundary-layer buildup within the rotor, tip clearance effect, or other reasons. These results indicate that the method of analysis used herein was found to predict accurately the over-all turbine performance over a wide range of speeds and pressure ratios and failed only in the region of the turbine limiting loading point. The good agreement further suggests that the analytical breakdown of the turbine losses can be considered fairly representative of the actual breakdown of losses.

Nozzle and rotor effective viscous losses. - The effect of the nozzle and rotor effective viscous losses on the analytically obtained turbine efficiency is shown in figure 4. These losses represent all losses other than incidence losses, exit whirl losses, and shock losses. They thus include secondary flow losses, tip clearance losses, and actual

blade viscous losses. Although these losses probably vary over the map, the close agreement of the analytical and experimental rating efficiencies indicates that assuming an effective viscous loss in accordance with the assumptions used in the analysis yields reasonable results.

At each of the five speeds, the efficiency, considering the effective viscous loss only, increases as the specific work output is increased and can be attributed to the higher level of specific work output. The efficiency variation occurring as a result of effective viscous loss ranges between 0.79 and 0.89.

Rotor incidence loss. - The rotor incidence loss was found to have a pronounced effect on the efficiency over the performance map. At 40 percent design speed and high specific work outputs (fig. 4(a)), the rotor incidence loss is seen to contribute greatly to the low turbine efficiency and represents as much as 18 points loss in efficiency. This high loss is due to a combination of high positive angle of incidence and high relative critical velocity ratio. At speeds approaching design the incidence loss is small, since the angle of incidence is low. At 120 percent design speed (fig. 4(e)), the drop in efficiency due to incidence loss is again large (as much as 15 points), but occurs at a low specific work output. The large loss in efficiency in this region is mainly due to the combination of the low work level and high incidence angle.

Rotor exit shock loss. - In the calculations, it was assumed that a normal shock loss corresponding to the supersonic velocity at station 5 (fig. 1) occurred. This is probably greater than would actually exist in the turbine, as a series of oblique shocks would be more likely (see ref. 4, for example). From figure 4, however, it can be concluded that over the entire performance map, a loss in efficiency due to shock is very small and can be attributed to the following: (a) The shock loss occurs only at high specific work output levels, and (b) limiting loading is reached before the velocities at station 5 become excessive.

Exit whirl loss. - As would be expected, the exit whirl loss varies considerably over the performance map. At low-speed high specific work outputs, the whirl loss represents as much as 13 points loss in efficiency. At intermediate speeds, the loss decreases substantially because the flow is close to axial. Then again at high-speed low pressure ratios, the loss due to whirl is large.

#### Variation in Rotor Mean Angle of Incidence and Relative Critical Velocity Ratio over Performance Map

The rotor incidence loss was found to have a marked effect on the off-design characteristics of the turbine. It is therefore of interest to study



the variation in incidence angle and relative critical velocity ratio over the range of performance investigated, since the loss is a function of both these variables. Figures 5 and 6 are again the analytically obtained performance map showing contours of calculated rotor entrance critical velocity ratio and angle of incidence. The velocity ratio (fig. 5) is seen to vary considerably over the performance range, from 0.80 at low-speed high pressure ratios to a value approaching 0.40 at high-speed low pressure ratios. The velocity ratio contours are vertical after the rotor chokes because conditions then remain fixed at the rotor entrance. It might be noted that the relative critical velocity ratio would be considerably greater at the hub and would probably exceed sonic conditions at low-speed high pressure ratios.

In figure 6 is the performance map with contours of constant relative angle of incidence. An extremely large variation in angle of incidence is seen to occur over the map, from  $30^\circ$  at low-speed high pressure ratios to  $-40^\circ$  at high-speed low pressure ratios. The effect of the angle of incidence in combination with the critical velocity ratio on the efficiency was shown in the previous section to be pronounced.

#### DISCUSSION

The method of analysis used herein was found to be satisfactory in predicting the off-design performance of the subject turbine. The results of the analytical investigation indicated that the decrease in efficiency at low-speed high pressure ratios and at high-speed low pressure ratios is due mainly to rotor incidence and turbine exit whirl losses. Thus, it can be concluded that if a turbine must operate efficiently at more than one condition, the turbine design must be a compromise between turbine exit whirl and angle of incidence to obtain an optimum design. For example, at low speeds, the rotor incidence loss was found to have a large effect on the turbine efficiency. Hence, if favorable acceleration characteristics were desired, improvements in efficiency at the low speeds could be obtained by designing the turbine for a negative angle of incidence at the design point. The small drop in efficiency at the design point due to the negative incidence angle would be off-set by a considerable improvement in efficiency at the lower speeds.

The loss in efficiency due to shock at the rotor exit was found in the analysis to be very small. However, provision for shock losses should be included in the analysis, since in the calculations, although the loss is small, it can shift the limiting loading point to a certain extent.

The one large disadvantage of the method used herein, as also occurred for the method in reference 2, is that the efficiency at one

point on the performance map must either be known or estimated in order to obtain the effective viscous loss parameter  $K$ . However, for a well-designed conventional turbine, the loss parameter  $K$  can be evaluated on the basis of an estimated rating efficiency between 0.87 and 0.90, and the result should be close to that expected experimentally.

It might be mentioned that the application of the flow chart and general procedure can be used with experimental loss parameters determined from cascade studies. The calculations involving the functions of  $K$  would then be replaced by the blade experimentally obtained losses. The difficulty with this is that (a) the loss distribution through the blade would still have to be assumed, and (b) if the losses are obtained from cascade results, there is no assurance that the blade would have similar losses in the actual turbine.

#### SUMMARY OF RESULTS

The performance of a turbine was obtained analytically to study the variation of losses over the performance map. The results of the analysis are compared with the experimental results to evaluate the analytical method. The results of the investigation are summarized as follows:

(1) Good correlation between the analytically and experimentally obtained performance was found over the entire map until limiting loading was approached. The discrepancy near limiting loading was apparently due to the fact that the blade effective throat area was not equal to the physical throat area.

(2) The results of the analysis indicated that the decrease in efficiency at low-speed high pressure ratios and at high-speed low pressure ratios was due primarily to rotor inlet incidence and turbine exit whirl losses.

(3) Rotor exit shock losses were found to have only a small effect on the analytically determined rating efficiency.

(4) Rotor mean incidence angles from  $-40^\circ$  to  $30^\circ$  and relative critical velocity ratios from 0.40 to 0.80 were found over the range of performance investigated. The combination of these variables caused the large incidence losses at off-design operating conditions.

Lewis Flight Propulsion Laboratory  
National Advisory Committee for Aeronautics  
Cleveland, Ohio, November 10, 1953

## APPENDIX A

## SYMBOLS

The following symbols are used in this report:

A	flow area, sq ft
a	effective viscous loss parameter due to blade inlet velocity (see ref. 2) $\left\{ 1 - K \left( \frac{p}{p_i} \right)^{\frac{1}{\gamma}} \left[ 1 - \left( \frac{p}{p_i} \right)^{\frac{\gamma-1}{\gamma}} \right] \right\}$
b	effective viscous loss parameter due to blade exit velocity (see ref. 2) $\left\{ 1 + K \left( \frac{p}{p_i} \right)^{\frac{1}{\gamma}} \left[ 1 - \left( \frac{p}{p_i} \right)^{\frac{\gamma-1}{\gamma}} \right] \right\}$
$c_p$	specific heat at constant pressure, Btu/lb/°R
$c_v$	specific heat at constant volume, Btu/lb/°R
h	specific enthalpy, Btu/lb
i	incidence angle, deg (see fig. 1)
K	blade effective loss parameter (ref. 2)
N	rotational speed, rpm
p	pressure, lb/sq ft
r	radius, ft
T	absolute temperature, °R
U	mean blade velocity, ft/sec
V	absolute gas velocity, ft/sec
W	relative gas velocity, ft/sec
w	weight flow rate, lb/sec
$\gamma$	ratio of specific heats, $c_p/c_v$

$\delta$  ratio of inlet air pressure to NACA standard sea-level pressure,  
 $p_0'/p^*$

$\epsilon$  function of  $r, \frac{r^*}{r} \left[ \frac{\left(\frac{r+1}{2}\right)^{\frac{r}{r-1}}}{\left(\frac{r^*+1}{2}\right)^{\frac{r^*}{r^*-1}}} \right]$

$\eta$  efficiency

$\theta_{cr}$  squared ratio of critical velocity at turbine inlet to critical  
 velocity at NACA standard sea-level temperature,  $(v_{cr}/v_{cr}^*)^2$

$\theta_{r,1}$  rotor inlet blade angle at mean radius (see fig. 1)

$\theta_2$  defines angle  $\sin^{-1} (A_1/A_2)$

$\xi$  shock loss corresponding to velocity at station 2 or 5 expressed  
 as total-pressure ratio

$\rho$  gas density, lb/cu ft

Subscripts:

ac above choking conditions

ann annulus

c choking conditions

cr conditions at Mach number of unity

isen isentropic

m mean radius

r relative

t tip, tangent to mean camber line

u tangential component

x axial component

- 0 nozzle inlet (fig. 1)
- 1 nozzle throat
- 2 station just inside nozzle trailing edge
- 3 nozzle exit, rotor entrance
- 4 rotor throat
- 5 station just inside rotor trailing edge
- 6 rotor exit, turbine exit

Superscripts:

- ' absolute total state
- " relative total state
- \* NACA standard conditions

## APPENDIX B

## CHARTS, GRAPHS, AND TABLE USED IN PERFORMANCE CALCULATION

Flow chart. - A most useful chart for obtaining flow conditions at a point is shown in figure 7. This chart relates the three velocity components and specific weight flow in a nondimensional manner. The equations used in the construction of the chart are

$$\frac{\rho V_x}{\rho' V_{cr}} = \frac{V_x}{V_{cr}} \left\{ 1 - \frac{\gamma-1}{\gamma+1} \left[ \left( \frac{V_x}{V_{cr}} \right)^2 + \left( \frac{V_u}{V_{cr}} \right)^2 \right] \right\}^{\frac{1}{\gamma-1}} \quad (B1)$$

and

$$\left( \frac{V}{V_{cr}} \right)^2 = \left( \frac{V_x}{V_{cr}} \right)^2 + \left( \frac{V_u}{V_{cr}} \right)^2 \quad (B2)$$

The chart is for a  $\gamma = 1.4$  and has already been presented in a number of reports (ref. 5, e.g.). The curves shown on figure 7 will be discussed later.

Incidence loss graph. - Figure 8 shows the pressure loss as a function of incidence angle for lines of constant critical velocity ratio. This graph was obtained as follows: For a given  $(W/W_{cr})_3$  a series of incidence angles was assumed and a value of  $(W_t/W_{cr})_3$  (component of relative critical velocity ratio in direction of rotor mean camber line) was then obtained by use of the relation

$$\left( \frac{W_t}{W_{cr}} \right)_3 = \left( \frac{W}{W_{cr}} \right)_3 \cos i \quad (B3)$$

For each value of  $(W/W_{cr})_3$  and  $(W_t/W_{cr})_3$ , values of  $(p/p'')_3$  were obtained from reference 6. Finally, the pressure loss due to incidence angle was obtained by the relation

$$\left( \frac{p_t''}{p''} \right)_3 = \frac{\left( \frac{p}{p''} \right)_3}{\left( \frac{p}{p_t''} \right)_3} \quad (B4)$$

Pressure ratio enthalpy drop table. - Table I shows the total enthalpy drop as a function of total-pressure ratio  $p'_0/p'_6$ . It was obtained for  $\gamma = 1.4$  from the following equation using standard inlet conditions:

$$\frac{\Delta h'}{\theta_{cr}} = c_p T^* \left[ 1 - \left( \frac{p'_6}{p'_0} \right)^{\frac{\gamma-1}{\gamma}} \right]$$

where, for the table,

$$c_p = 0.24$$

$$T^* = 518.4^\circ \text{ R}$$

$$\gamma = 1.4$$

## APPENDIX C

## NOZZLE AND ROTOR OPERATING CURVES

Before beginning the actual performance calculations, it is beneficial to obtain a series of working curves.

Effective viscosity loss curves. - When the value of the effective viscosity loss parameter  $K$  is known, a curve similar to that shown in figure 9 can be constructed using the following equations, which relate the total-pressure loss parameters  $a$  and  $b$  to the total-to-static pressure ratio at the blade inlet and exit, respectively,

$$a = 1 - K \left( \frac{p}{p_t} \right)^{\frac{1}{\gamma}} \left[ 1 - \left( \frac{p}{p_t} \right)^{\frac{\gamma-1}{\gamma}} \right] \quad (C1)$$

$$b = 1 + K \left( \frac{p}{p_t} \right)^{\frac{1}{\gamma}} \left[ 1 - \left( \frac{p}{p_t} \right)^{\frac{\gamma-1}{\gamma}} \right] \quad (C2)$$

(See ref. 2 for derivations.) Figure 9 shows these parameters as a function of the critical velocity ratio for convenience of use. The relation between critical velocity ratio and total-to-static pressure ratio was obtained from reference 6.

Blade throat and exit flow curves. - The nozzle and rotor throat and exit flow conditions are superimposed on the flow chart of figure 7. These curves are obtained as follows.

For a given blade row, for example, the nozzle blade row, the throat area  $A_1$ , axial flow area just inside the trailing edge  $A_2$ , and free-stream annulus area downstream of the blade row  $A_3$  must first be obtained from the turbine geometry. After defining

$$\theta_2 = \sin^{-1} \frac{A_1}{A_2} \quad (C3)$$

it is assumed that the flow follows the angle  $\theta_2$  at station 2 until the blade row chokes,  $(V/V_{cr})_2 = 1$ . Hence, for assumed values of  $(V/V_{cr})_2$ ,  $(V_u/V_{cr})_2$  can be obtained from the relation

$$\left( \frac{V_u}{V_{cr}} \right)_2 = \left( \frac{V}{V_{cr}} \right)_2 \cos \theta_2 \quad (C4)$$



Curve A-B can then be plotted on figure 7 up to  $(V/V_{cr})_2 = 1$ . It is then assumed that

$$\left(\frac{V_u}{V_{cr}}\right)_2 = \left(\frac{V_u}{V_{cr}}\right)_3 \quad (C5)$$

and from continuity, assuming no losses between stations 2 and 3,

$$\left(\frac{\rho V_x}{\rho' V_{cr}}\right)_3 = \left(\frac{\rho V_x}{\rho' V_{cr}}\right)_2 \times \frac{A_2}{A_3} \quad (C6)$$

Hence, curve C-D can also be plotted using equations (C5) and (C6).

For  $(V/V_{cr})_2 > 1$ , the loss parameter  $b$  corresponding to  $(V/V_{cr})_3$  and shock loss corresponding to  $(V/V_{cr})_2$  must be considered in the calculations. The total-pressure drop across a blade row due to the effective viscous loss is assumed to be dependent on  $(V/V_{cr})_0$  and  $(V/V_{cr})_3$ . However, once the blade is choked, any additional pressure drop is felt downstream of the throat only. After the blade chokes,

$$w = \text{constant}$$

So at station 2,

$$(\rho V_x)_{2,c} = (\rho V_x)_{2,ac} \quad (C7)$$

and

$$\left(\frac{\rho V_x}{\rho' V_{cr}}\right)_{2,ac} = \left(\frac{\rho V_x}{\rho' V_{cr}}\right)_{2,c} \times \frac{b_{3,ac}}{b_{3,c}} \times \frac{1}{\xi} \quad (C8)$$

A series of  $(V/V_{cr})_2$  is assumed to obtain the supersonic portion of the curves. Then for each  $(V/V_{cr})_2$  a series of  $b_3$  is assumed. With the use of equation (C8) and the known condition at the choking point,  $(\rho V_x / \rho' V_{cr})_2$  can be computed and  $(V_u / V_{cr})_2$  can be obtained from figure 7. Conditions at station 3 can then be determined with the aid of equations (C5) and (C6). The  $b_3$  assumed and the  $b_3$  obtained from figure 9 and conditions at station 3 must be the same. Hence, the supersonic portion of the curves can then be plotted. For the turbine analyzed herein, supersonic conditions at the nozzle exit were not encountered. Hence, these curves are not shown. Curves E-F and G-H are the supersonic portions of the rotor curves at stations 5 and 6, respectively. Curve J-K presents the operating curve for the rotor and nozzle throat in the direction of flow.

Nozzle effective viscosity loss curve. - The nozzle total-pressure ratio  $a_0/b_3$  resulting from the nozzle effective viscosity loss can be obtained as a function of  $(V_u/V_{cr})_2$ . For a given  $(V_u/V_{cr})_2$  and the working curve (fig. 7),  $(V/V_{cr})_3$  can be obtained. This value is then used to determine  $b_3$  from figure 9. Continuity is then used to obtain  $a_0$ . Assuming a range of  $a_0$ ,  $(\rho V_x/\rho' V_{cr})_0$  is obtained from the equation

$$\left( \frac{\rho V_x}{\rho' V_{cr}} \right)_0 = \left( \frac{\rho V_x}{\rho' V_{cr}} \right)_3 \times \frac{A_3}{A_0} \times \frac{a_0}{b_3} \quad (C9)$$

Since  $(V_u/V_{cr})_0 = 0$  at the nozzle entrance, the working curve for station 0 is curve J-K (fig. 7). Hence, figure 7 and  $(\rho V_x/\rho' V_{cr})_0$  can be used to obtain  $(V/V_{cr})_0$ . The assumed  $a_0$  should then check the  $a_0$  corresponding to  $(V/V_{cr})_0$  (fig. 9). The nozzle effective viscosity loss curve for the turbine analyzed herein is shown in figure 10.

It might be noted that a working curve such as that shown in figure 10 cannot be used for a blade row having a varying inlet flow angle (such as a rotor or the second stage nozzle).

## APPENDIX D

## SAMPLE CALCULATION

The analysis of the turbine investigated in this report at one operating point will be presented here to illustrate the method used in the performance calculation. The point chosen was that point where the rotor choked at 100 percent design speed.

Nozzle exit conditions. - For a given speed a series of  $(V_u/V_{cr})_2$  is assumed and the performance calculated until  $(W/W_{cr})_4 = 1$ . At this point, for 100 percent design speed,

$$\left(\frac{V_u}{V_{cr}}\right)_2 = 0.768 \quad (D1)$$

Then

$$\left(\frac{V_x}{V_{cr}}\right)_3 = 0.528 \text{ (fig. 7)} \quad (D2)$$

$$\frac{a_0}{b_3} = 0.9533 \text{ (fig. 10)} \quad (D3)$$

Rotor inlet conditions. - For 100 percent design speed,

$$\left(\frac{U}{V_{cr}}\right)_3 = 0.620 \quad (D4)$$

The relation between relative and absolute total temperature in terms of absolute quantities can be expressed as

$$\frac{T''}{T'} = 1 - \frac{\gamma-1}{\gamma+1} \left(\frac{U}{V_{cr}}\right) \left(2 \frac{V_u}{V_{cr}} - \frac{U}{V_{cr}}\right)$$

Hence, using (D1), (D4), and  $\gamma = 1.4$  in the preceding equation gives

$$(T''/T')_3 = 0.905 \quad (D5)$$

Now

$$\begin{aligned}
 \left( \frac{W_u}{V_{cr}} \right)_3 &= \left( \frac{V_u}{V_{cr}} \right)_3 - \left( \frac{U}{V_{cr}} \right)_3 \\
 &= 0.768 - 0.620 \\
 &= 0.148
 \end{aligned} \tag{D6}$$

So, from trigonometry and equations (D2) and (D6),

$$\left( \frac{W}{V_{cr}} \right)_3 = 0.549 \tag{D7}$$

The component of relative velocity normal to the blade entrance angle is assumed lost as an incidence loss (same assumption as in ref. 2). For the turbine analyzed herein,

$$\theta_{r,i} = 15.4^\circ \tag{D8}$$

thus

$$i = \tan^{-1} \frac{\left( \frac{W_u}{V_{cr}} \right)_3}{\left( \frac{V_x}{V_{cr}} \right)_3} - 15.4^\circ$$

Using (D2) and (D6) gives

$$\begin{aligned}
 i &= \tan^{-1} \frac{0.148}{0.528} - 15.4^\circ \\
 &= 0.3^\circ
 \end{aligned} \tag{D9}$$

Now

$$\begin{aligned}
 \left( \frac{W}{V_{cr}} \right)_3 &= \left( \frac{W}{V_{cr}} \right)_3 \times \left( \frac{V_{cr}}{W_{cr}} \right)_3 \\
 &= \frac{\left( \frac{W}{V_{cr}} \right)_3}{\left( \frac{T''}{T'} \right)_3^{1/2}}
 \end{aligned}$$

Equations (D7) and (D5) yield

$$\left(\frac{W}{W_{cr}}\right)_3 = 0.576 \quad (D10)$$

Now

$$\left(\frac{W_t}{W_{cr}}\right)_3 = \left(\frac{W}{W_{cr}}\right)_3 \cos i$$

By use of equations (D9) and (D10),

$$\left(\frac{W_t}{W_{cr}}\right)_3 = 0.576 \quad (D11)$$

Using figure 8 and equations (D9) and (D10) gives

$$\left(\frac{p_t''}{p''}\right)_3 = 1 \quad (D12)$$

Figure 9 and equation (D11) give

$$a_{r,3} = 0.981 \quad (D13)$$

Rotor exit conditions. - For the turbine being analyzed, the mean radius ratio changed from 0.84 at the rotor entrance to 0.805 at the rotor exit; thus

$$\frac{U_6}{U_3} = \frac{0.805}{0.84} = 0.958 \quad (D14)$$

Because the turbine mean radius ratio decreases from inlet to exit, there is a relative total-temperature drop expressible by the following equation:

$$\frac{T_3'' - T_6''}{T_3'} = \frac{\gamma-1}{\gamma+1} \left(\frac{U}{V_{cr}}\right)_3^2 \left[1 - \left(\frac{U_6}{U_3}\right)^2\right]$$

Hence, using this equation, (D4), (D14), and  $\gamma = 1.4$  gives

$$\frac{T_3'' - T_6''}{T_3'} = 0.005$$

3076

Using (D5) results in

$$\begin{aligned}\frac{T_6''}{T_3'} &= 0.905 - 0.005 \\ &= 0.900\end{aligned}\quad (D15)$$

Continuity between stations 1 and 4 is used to calculate the rotor exit conditions.

$$w = (\rho VA)_1 = (\rho WA)_4$$

$$(\rho W)_4 = (\rho V)_1 \left( \frac{A_1}{A_4} \right)$$

$$\left( \frac{\rho W}{\rho'' W_{cr}} \right)_4 = \left( \frac{\rho V}{\rho' V_{cr}} \right)_1 \times \frac{A_1}{A_4} \times \left( \frac{\rho' V_{cr}}{\rho'' W_{cr}} \right)_1$$

Since  $\frac{T_6''}{T_3'} = \frac{T_4''}{T_1'}$ ,

$$\left( \frac{\rho W}{\rho'' W_{cr}} \right)_4 = \left( \frac{\rho V}{\rho' V_{cr}} \right)_1 \times \frac{A_1}{A_4} \times \left( \frac{T_6''}{T_3'} \right)^{1/2} \times \frac{p_1'}{p_4''} \quad (D16)$$

For this turbine

$$\frac{A_1}{A_4} = 0.690 \quad (D17)$$

Also, using equation (D1) and figure 7,

$$\left( \frac{V}{V_{cr}} \right)_2 = 0.955$$

Since the nozzle is not choked,

$$\left( \frac{V}{V_{cr}} \right)_1 = \left( \frac{V}{V_{cr}} \right)_2 = 0.955$$

Hence, figure 7 and the working curve for station 1 are used to find

$$\left( \frac{\rho V}{\rho' V_{cr}} \right)_1 = 0.632 \quad (D18)$$

The ratio of relative total pressure at station 4 to total pressure at station 1 can be written

$$\frac{p_4''}{p_1'} = \frac{a_{r,3}}{b_{r,6}} \times \left( \frac{p_t''}{p''} \right)_3 \times \left( \frac{T_6''}{T_1'} \right)^{\frac{\gamma}{\gamma-1}}$$

In this equation, everything is known except  $b_{r,6}$ . Various values of  $b_{r,6}$  are assumed to obtain  $(W/W_{cr})_6$ . The assumed  $b_{r,6}$  must check that obtained with  $(W/W_{cr})_6$  and figure 9. It was found that for this point

$$b_{r,6} = 1.040 \quad (D19)$$

So, using (D12), (D13), (D15), and (D19),

$$p_4''/p_1' = 0.653 \quad (D20)$$

Substituting (D15), (D17), (D18), and (D20) into (D16) gives

$$(\rho W/\rho'' W_{cr})_4 = 0.634 \quad (D21)$$

Figure 7 is used to find

$$(W/W_{cr})_4 = 1 \quad (D22)$$

$$(W/W_{cr})_6 = 0.947 \quad (D23)$$

$$(W_x/W_{cr})_6 = 0.648 \quad (D24)$$

$$(W_u/W_{cr})_6 = -0.692 \quad (D25)$$

Turbine exit conditions. - To begin the turbine exit calculations  $(W/W_{cr})_6$  is first found:

$$\left( \frac{U}{W_{cr}} \right)_6 = \left( \frac{U}{V_{cr}} \right)_3 \times \frac{U_6}{U_3} \times \frac{V_{cr,3}}{W_{cr,6}}$$

Using (D4), (D14), (D15), and  $\frac{V_{cr,3}}{W_{cr,6}} = \left( \frac{T_3}{T_6''} \right)^{1/2}$ ,

$$(U/W_{cr})_6 = 0.626 \quad (D26)$$

The ratio of absolute to relative total temperature in terms of relative quantities can be expressed as

$$\frac{T'}{T''} = 1 + \frac{\gamma-1}{\gamma+1} \left( \frac{U}{W_{cr}} \right)^2 \left( 2 \frac{W_u}{W_{cr}} + \frac{U}{W_{cr}} \right)$$

Using this equation, (D25), (D26), and  $\gamma = 1.4$

$$(T'/T'')_6 = 0.921 \quad (D27)$$

So

$$\left( \frac{V_{cr}}{W_{cr}} \right)_6 = \left( \frac{T'}{T''} \right)_6^{1/2} = 0.960 \quad (D28)$$

Using (D24), (D25), (D26), and (D28) gives

$$(V_u/W_{cr})_6 = 0.626 - 0.692$$

$$= -0.066$$

$$(V_u/V_{cr})_6 = -0.066/0.960 = -0.069 \quad (D29)$$

$$(V_x/V_{cr})_6 = 0.648/0.960 = 0.675 \quad (D30)$$

From trigonometry and equations (D29) and (D30),

$$(V/V_{cr})_6 = 0.677 \quad (D31)$$

Performance parameters. - (1) Specific work output: The equivalent specific work output is obtained from the following equation:

$$\frac{\Delta h'}{\theta_{cr}} = c_p T_0' \left( 1 - \frac{T'_6}{T_0'} \right)$$

and since standard inlet conditions were assumed,

$$T_0' = 518.4$$

$$c_p = 0.240$$



From equations (D15) and (D27),

$$\begin{aligned} T'_6/T'_0 &= 0.921 \times 0.900 \\ &= 0.829 \end{aligned}$$

Hence,

$$\frac{\Delta h'}{\theta_{cr}} = 21.28 \text{ Btu/lb} \quad (\text{D32})$$

(2) Total-pressure ratio based on axial component of velocity: Equations (D30) and (D31) and reference 6 give

$$(p/p')_6 = 0.758, (p/p'_x)_6 = 0.760 \quad (\text{D33})$$

Also,

$$\frac{p'_{x,6}}{p'_0} = \frac{p'_{x,6}}{p_6} \times \frac{p_6}{p'_6} \times \frac{p'_6}{p''_6} \times \frac{p''_6}{p''_4} \times \frac{p''_4}{p'_1} \times \frac{p'_1}{p'_0} \quad (\text{D34})$$

Since at unchoked rotor conditions  $p''_6 = p''_4$ , equations (D3), (D20), (D27), and (D33) can be used to obtain

$$\begin{aligned} p'_{x,6}/p'_0 &= 0.4649 \\ p'_0/p'_{x,6} &= 2.145 \end{aligned} \quad (\text{D35})$$

(3) Efficiency based on axial component of velocity: Table I presents the variation in the equivalent specific work output  $\Delta h'/\theta_{cr}$  with total-pressure ratio. This table and (D35) are used to find

$$(\Delta h'/\theta_{cr})_{isen} = 24.41 \text{ Btu/lb} \quad (\text{D36})$$

Hence, with (D32),

$$\eta_x = 21.3/24.4 = 0.87 \quad (\text{D37})$$

(4) Equivalent weight flow: Conditions at station 3 were used to obtain the equivalent weight flow.

$$\epsilon \frac{w\sqrt{\theta_{cr}}}{\delta} = \left( \frac{\rho V_x}{\rho' V_{cr}} \right)_3 \times (\rho' V_{cr})_3 \times A_3$$

From figure 7,

$$(\rho V_x / \rho' V_{cr})_3 = 0.358$$

With standard inlet conditions,

$$\begin{aligned} (\rho' V_{cr})_3 &= (\rho' V_{cr})_0 \times a_0 / b_3 \\ &= 0.0765 \times 1019 \times 0.9533 \\ &= 74.30 \end{aligned}$$

Also,

$$A_{ann,3} = 0.575 \text{ sq ft}$$

Hence,

$$\epsilon \frac{w \sqrt{\theta_{cr}}}{\delta} = 15.29 \text{ lb/sec} \quad (D38)$$

(5) Weight-flow - speed parameter: The weight-flow - speed parameter can be expressed as

$$\epsilon \frac{wN}{\delta} = \epsilon \frac{w \sqrt{\theta_{cr}}}{\delta} \times \frac{N}{\sqrt{\theta_{cr}}}$$

For this point,

$$N / \sqrt{\theta_{cr}} = 12,304 \text{ rpm}$$

So

$$\begin{aligned} \epsilon \frac{wN}{\delta} &= 12,304 \times 15.29 \\ &= 18.8 \times 10^4 \end{aligned}$$

Conditions above rotor choking point. - The calculations just described were for the rotor choking point. After the rotor has choked, all conditions upstream from the rotor throat are constant. Hence, a series of  $(W/W_{cr})_5$  can be assumed up to the limiting loading point. From the working curves on figure 7, the relative velocity components at station 6 can then be obtained and the calculations continued, starting with (D23). The value of  $b_{r,6}$  is obtained using  $(W/W_{cr})_6$  and figure 9, and the term  $\xi_5$  can be obtained from reference 6. So, rewriting (D34),

$$\frac{p'_{x,6}}{p'_0} = \left( \frac{p'_1}{p'_0} \times \frac{p''_4}{p'_1} \right) \frac{p''_6}{p''_4} \times \frac{p'_6}{p''_6} \times \frac{p_6}{p'_6} \times \frac{p'_{x,6}}{p_6}$$

Since

$$\frac{p''_6}{p''_4} = \frac{\xi_5(b_{r,6})_c}{b_{r,6}}$$

The value of  $p'_{x,6}/p'_0$  can then be obtained; otherwise, the method for calculating the performance is the same as just described.

## APPENDIX E

## METHOD OF OBTAINING EFFECT OF LOSSES ON TURBINE RATING EFFICIENCY

Presented in this appendix is a sample calculation to illustrate the method used in finding the effect of the various losses on the rating efficiency. The point used is again 100 percent design speed and the rotor choking point. From appendix D,

$$\Delta h' / \theta_{cr} = 21.28 \text{ Btu/lb} \quad (D32)$$

From table I,

$$(p'_0/p'_6)_{isen} = 1.9295 \quad (D33)$$

This corresponds to  $\eta = 1.00$ , since no losses have been introduced.

Efficiency including nozzle effective viscous loss. -

$$p'_0/p'_6 = (p'_0/p'_6)_{isen} b_3/a_0$$

Equations (D3) and (D33) are used to find

$$\begin{aligned} p'_0/p'_6 &= 1.9295 \times 1/0.9533 \\ &= 2.024 \end{aligned} \quad (E1)$$

From table I,

$$(\Delta h' / \theta_{cr})_{isen} = 22.67$$

So

$$\eta = 21.28/22.67$$

$$\eta = 0.939$$

Efficiency including losses up to and including incidence loss. -

$$\frac{p'_0}{p'_6} = \left[ \left( \frac{p'_0}{p'_6} \right)_{isen} \times \frac{b_3}{a_0} \right] \times \left( \frac{p''}{p_t} \right)_3$$

From equations (E1) and (D12)

$$\begin{aligned} (p'_0/p'_6) &= 2.024 \times 1 \\ &= 2.024 \end{aligned} \quad (E2)$$

$$(\Delta h'/\theta_{cr})_{isen} = 22.66$$

$$\eta = 21.28/22.67$$

$$\eta = 0.939$$

Efficiency including losses up to and including rotor affecting viscous loss. -

$$\frac{p'_0}{p'_6} = \left[ \left( \frac{p'_0}{p'_6} \right)_{isen} \times \frac{b_3}{a_0} \times \left( \frac{p''}{p'_t} \right)_3 \right] \times \frac{b_{r,6}}{a_{r,3}}$$

By use of equations (E2), (D13), and (D19),

$$\begin{aligned} p'_0/p'_6 &= 2.024 \times 1.040/0.9810 \\ &= 2.146 \end{aligned} \quad (E3)$$

$$(\Delta h'/\theta_{cr})_{isen} = 24.35$$

$$\eta = 21.28/24.35$$

$$\eta = 0.874$$

Efficiency including losses up to and including rotor shock losses. -  
Since the rotor is just choked, there is no shock loss at this point. Above the rotor choking point, however, the shock loss would be calculated, and the efficiency including this loss would then be obtained at this point in the calculations.

Efficiency including losses up to and including exit whirl loss. -

$$\frac{p'_0}{p'_6} = \left[ \left( \frac{p'_0}{p'_6} \right)_{isen} \times \frac{b_3}{a_0} \times \left( \frac{p''}{p'_t} \right)_3 \times \frac{b_{r,6}}{a_{r,3}} \times \frac{1}{\xi} \right] \times \frac{p'_{x,6}}{p'_6}$$

From (E3) and (D33),

$$p'_0/p'_6 = 2.146 \times 0.760/0.758$$

$$= 2.152$$

$$(\Delta h'/\theta_{cr})_{isen} = 24.43 \text{ Btu/lb}$$

$$\eta = 21.28/24.43$$

$$\eta = 0.871$$

This is the rating efficiency and should check the calculations previously made pertaining to the performance map.

#### REFERENCES

1. Whitney, Warren J., Stewart, Warner L., and Schum, Harold J.: Investigation of Turbines for Driving Supersonic Compressors. IV - Design and Performance of Second Configuration Including Study of Three-Dimensional Flow Effects. NACA RM E53C02, 1953.
2. Kochendorfer, Fred D., and Nettles, J. Cary: An Analytical Method of Estimating Turbine Performance. NACA Rep. 930, 1949. (Supersedes NACA RM E8I16.)
3. English, Robert E., and Cavicchi, Richard H.: Comparison of Measured Efficiencies of Nine Turbine Designs with Efficiencies Predicted by Two Empirical Methods. NACA RM E51F13, 1951.
4. Hauser, Cavour H., and Flohr, Henry W.: Two-Dimensional Cascade Investigation of the Maximum Exit Tangential Velocity Component and other Flow Conditions at the Exit of Several Turbine Blade Designs at Supercritical Pressure Ratios. NACA RM E51F12, 1951.
5. Alpert, Sumner, and Litrenta, Rose M.: Construction and Use of Charts in Design Studies of Gas Turbines. NACA TN 2402, 1951.
6. The Staff of the Ames 1- by 3-Foot Supersonic Wind-Tunnel Section: Notes and Tables for Use in the Analysis of Supersonic Flow. NACA TN 1428, 1947.

TABLE I. -- TABULATION OF CORRECTED ENTHALPY DROP FOR VARIOUS VALUES OF  
PRESSURE RATIO (FOR  $\gamma = 1.4$ )

$\frac{p_0}{p_6} \rightarrow$	$\Delta h' / \theta_{cr}$									
	0	.001	.002	.003	.004	.005	.006	.007	.008	.009
1.25	7.67	7.70	7.72	7.75	7.78	7.80	7.83	7.86	7.89	7.91
1.26	7.94	7.97	7.99	8.02	8.04	8.07	8.10	8.13	8.15	8.18
1.27	8.21	8.24	8.26	8.29	8.31	8.34	8.36	8.39	8.42	8.44
1.28	8.47	8.50	8.52	8.55	8.57	8.60	8.62	8.65	8.68	8.70
1.29	8.73	8.75	8.78	8.80	8.83	8.85	8.88	8.90	8.93	8.96
1.30	8.98	9.01	9.03	9.06	9.08	9.11	9.14	9.16	9.19	9.21
1.31	9.24	9.26	9.29	9.31	9.34	9.36	9.39	9.42	9.44	9.46
1.32	9.49	9.51	9.54	9.56	9.59	9.62	9.64	9.66	9.69	9.71
1.33	9.74	9.76	9.79	9.81	9.84	9.86	9.88	9.91	9.93	9.96
1.34	9.98	10.00	10.03	10.05	10.08	10.10	10.12	10.15	10.17	10.20
1.35	10.22	10.24	10.27	10.29	10.32	10.34	10.36	10.39	10.41	10.44
1.36	10.46	10.48	10.51	10.53	10.56	10.58	10.60	10.63	10.65	10.68
1.37	10.70	10.72	10.75	10.77	10.79	10.81	10.84	10.86	10.88	10.91
1.38	10.93	10.95	10.98	11.00	11.02	11.05	11.07	11.10	11.12	11.14
1.39	11.16	11.19	11.21	11.23	11.26	11.28	11.31	11.33	11.35	11.37
1.40	11.39	11.42	11.44	11.46	11.49	11.51	11.54	11.56	11.58	11.60
1.41	11.62	11.65	11.67	11.69	11.71	11.74	11.76	11.78	11.81	11.83
1.42	11.85	11.87	11.89	11.92	11.94	11.96	11.98	12.00	12.03	12.05
1.43	12.07	12.09	12.11	12.14	12.16	12.18	12.20	12.22	12.25	12.27
1.44	12.29	12.31	12.33	12.36	12.38	12.40	12.42	12.44	12.47	12.49
1.45	12.51	12.53	12.55	12.58	12.60	12.62	12.64	12.66	12.69	12.71
1.46	12.73	12.75	12.77	12.80	12.82	12.84	12.86	12.88	12.91	12.93
1.47	12.95	12.97	12.99	13.02	13.04	13.06	13.08	13.10	13.13	13.15
1.48	13.17	13.19	13.21	13.23	13.25	13.28	13.30	13.32	13.34	13.36
1.49	13.38	13.40	13.42	13.44	13.46	13.49	13.51	13.53	13.55	13.57
1.50	13.59	13.61	13.63	13.65	13.67	13.70	13.72	13.74	13.76	13.78
1.51	13.80	13.82	13.84	13.86	13.88	13.90	13.93	13.95	13.97	13.99
1.52	14.01	14.03	14.05	14.07	14.09	14.12	14.14	14.16	14.18	14.20
1.53	14.22	14.24	14.26	14.28	14.30	14.32	14.34	14.36	14.38	14.40
1.54	14.43	14.45	14.47	14.49	14.51	14.53	14.55	14.57	14.59	14.61
1.55	14.63	14.65	14.67	14.69	14.71	14.73	14.75	14.77	14.79	14.81
1.56	14.83	14.85	14.87	14.89	14.91	14.93	14.95	14.97	14.99	15.01
1.57	15.03	15.05	15.07	15.09	15.11	15.13	15.15	15.17	15.19	15.21
1.58	15.23	15.25	15.27	15.29	15.31	15.33	15.35	15.37	15.39	15.41
1.59	15.43	15.45	15.47	15.49	15.51	15.53	15.55	15.57	15.59	15.61
1.60	15.63	15.65	15.67	15.69	15.71	15.72	15.74	15.76	15.78	15.80
1.61	15.82	15.84	15.86	15.88	15.90	15.91	15.93	15.95	15.97	15.99
1.62	16.01	16.03	16.05	16.07	16.09	16.11	16.12	16.14	16.16	16.18
1.63	16.20	16.22	16.24	16.26	16.28	16.30	16.31	16.33	16.35	16.37
1.64	16.39	16.41	16.43	16.45	16.47	16.49	16.50	16.52	16.54	16.56

TABLE I. - Continued. TABULATION OF CORRECTED ENTHALPY DROP FOR VARIOUS  
VALUES OF PRESSURE RATIO (FOR  $\gamma = 1.4$ )

$\frac{p_0}{p_6}$ ↓	$\Delta h' / \theta_{cr}$									
	0	.001	.002	.003	.004	.005	.006	.007	.008	.009
1.65	16.58	16.60	16.62	16.64	16.66	16.68	16.69	16.71	16.73	16.75
1.66	16.77	16.79	16.81	16.83	16.85	16.86	16.88	16.90	16.92	16.94
1.67	16.96	16.98	16.99	17.01	17.03	17.05	17.07	17.09	17.10	17.12
1.68	17.14	17.16	17.18	17.19	17.21	17.23	17.25	17.27	17.28	17.30
1.69	17.32	17.33	17.35	17.37	17.39	17.40	17.42	17.44	17.46	17.47
1.70	17.49	17.51	17.52	17.54	17.56	17.57	17.59	17.61	17.63	17.64
1.71	17.66	17.68	17.69	17.71	17.73	17.74	17.76	17.78	17.80	17.81
1.72	17.83	17.85	17.86	17.88	17.90	17.92	17.93	17.95	17.97	17.98
1.73	18.00	18.02	18.04	18.05	18.07	18.09	18.11	18.13	18.14	18.16
1.74	18.18	18.20	18.21	18.23	18.25	18.26	18.28	18.30	18.32	18.33
1.75	18.35	18.37	18.39	18.40	18.42	18.43	18.45	18.47	18.49	18.50
1.76	18.52	18.54	18.56	18.57	18.59	18.60	18.62	18.64	18.66	18.67
1.77	18.69	18.71	18.73	18.74	18.76	18.78	18.80	18.81	18.83	18.84
1.78	18.86	18.88	18.90	18.91	18.93	18.95	18.97	18.99	19.00	19.02
1.79	19.04	19.06	19.07	19.09	19.11	19.12	19.14	19.16	19.18	19.19
1.80	19.21	19.23	19.24	19.26	19.28	19.29	19.31	19.33	19.35	19.36
1.81	19.38	19.40	19.41	19.43	19.44	19.46	19.48	19.49	19.51	19.52
1.82	19.54	19.56	19.57	19.59	19.61	19.63	19.64	19.66	19.68	19.69
1.83	19.71	19.73	19.74	19.76	19.78	19.80	19.81	19.83	19.85	19.86
1.84	19.88	19.89	19.91	19.93	19.94	19.96	19.98	19.99	20.01	20.02
1.85	20.04	20.06	20.07	20.09	20.10	20.12	20.14	20.15	20.17	20.18
1.86	20.20	20.22	20.24	20.25	20.26	20.28	20.30	20.31	20.33	20.34
1.87	20.36	20.38	20.40	20.41	20.42	20.44	20.46	20.47	20.49	20.50
1.88	20.52	20.54	20.55	20.57	20.58	20.60	20.62	20.63	20.65	20.66
1.89	20.68	20.70	20.71	20.73	20.74	20.76	20.78	20.79	20.80	20.82
1.90	20.84	20.85	20.86	20.88	20.89	20.91	20.93	20.94	20.96	20.97
1.91	20.99	21.00	21.02	21.03	21.05	21.06	21.08	21.09	21.11	21.12
1.92	21.14	21.15	21.17	21.18	21.20	21.22	21.23	21.24	21.26	21.27
1.93	21.29	21.30	21.32	21.33	21.35	21.36	21.38	21.39	21.41	21.42
1.94	21.44	21.45	21.47	21.48	21.50	21.52	21.53	21.54	21.56	21.57
1.95	21.59	21.60	21.62	21.63	21.65	21.66	21.67	21.69	21.71	21.72
1.96	21.73	21.75	21.76	21.78	21.79	21.81	21.82	21.84	21.86	21.87
1.97	21.88	21.90	21.91	21.93	21.94	21.96	21.97	21.99	22.01	22.02
1.98	22.03	22.05	22.06	22.08	22.09	22.11	22.12	22.14	22.16	22.17
1.99	22.18	22.20	22.21	22.23	22.24	22.26	22.27	22.29	22.30	22.32
2.00	22.33	22.34	22.36	22.37	22.39	22.40	22.41	22.43	22.44	22.46
2.01	22.47	22.48	22.50	22.51	22.53	22.54	22.55	22.57	22.58	22.60
2.02	22.61	22.62	22.64	22.65	22.67	22.68	22.70	22.71	22.72	22.74
2.03	22.75	22.77	22.78	22.80	22.81	22.83	22.84	22.85	22.87	22.89
2.04	22.90	22.91	22.93	22.94	22.96	22.97	22.99	23.01	23.03	23.03



TABLE I. - Continued. TABULATION OF CORRECTED ENTHALPY DROP FOR VARIOUS  
VALUES OF PRESSURE RATIO (FOR  $\gamma = 1.4$ )

$\frac{p_0}{p_6}$	$\Delta h' / \theta_{cr}$									
	0	.001	.002	.003	.004	.005	.006	.007	.008	.009
2.05	23.04	23.05	23.07	23.08	23.10	23.11	23.12	23.14	23.15	23.17
2.06	23.18	23.19	23.21	23.22	23.24	23.25	23.26	23.28	23.29	23.30
2.07	23.32	23.33	23.35	23.36	23.37	23.38	23.40	23.41	23.42	23.44
2.08	23.45	23.46	23.48	23.49	23.51	23.52	23.54	23.55	23.56	23.58
2.09	23.59	23.60	23.62	23.63	23.64	23.66	23.67	23.68	23.70	23.71
2.10	23.72	23.73	23.75	23.76	23.78	23.80	23.81	23.82	23.83	23.85
2.11	23.86	23.87	23.89	23.90	23.92	23.93	23.94	23.96	23.97	23.99
2.12	24.00	24.01	24.03	24.04	24.06	24.07	24.08	24.10	24.11	24.13
2.13	24.14	24.15	24.16	24.18	24.19	24.20	24.22	24.23	24.24	24.26
2.14	24.27	24.28	24.29	24.31	24.32	24.34	24.35	24.36	24.37	24.39
2.15	24.40	24.41	24.43	24.44	24.46	24.47	24.48	24.50	24.51	24.53
2.16	24.54	24.55	24.57	24.58	24.59	24.60	24.62	24.63	24.64	24.66
2.17	24.67	24.68	24.70	24.71	24.72	24.74	24.75	24.76	24.77	24.79
2.18	24.80	24.82	24.83	24.84	24.86	24.87	24.88	24.90	24.91	24.93
2.19	24.94	24.95	24.97	24.98	24.99	25.00	25.02	25.03	25.04	25.06
2.20	25.07	25.08	25.10	25.11	25.12	25.13	25.15	25.16	25.17	25.19
2.21	25.20	25.21	25.23	25.24	25.25	25.26	25.28	25.29	25.30	25.32
2.22	25.33	25.34	25.36	25.37	25.38	25.39	25.40	25.41	25.43	25.44
2.23	25.45	25.46	25.48	25.49	25.50	25.52	25.53	25.54	25.55	25.57
2.24	25.58	25.59	25.60	25.62	25.63	25.64	25.65	25.66	25.68	25.69
2.25	25.70	25.72	25.73	25.74	25.75	25.77	25.78	25.79	25.80	25.82
2.26	25.83	25.84	25.86	25.87	25.88	25.90	25.91	25.92	25.93	25.95
2.27	25.96	25.97	25.98	26.00	26.01	26.02	26.03	26.04	26.06	26.07
2.28	26.08	26.10	26.11	26.12	26.13	26.14	26.16	26.17	26.18	26.19
2.29	26.20	26.22	26.23	26.24	26.26	26.27	26.28	26.29	26.30	26.32
2.30	26.33	26.34	26.35	26.37	26.38	26.39	26.40	26.41	26.43	26.44
2.31	26.45	26.46	26.47	26.49	26.50	26.51	26.52	26.53	26.55	26.56
2.32	26.57	26.58	26.59	26.61	26.62	26.63	26.65	26.66	26.67	26.68
2.33	26.69	26.70	26.72	26.73	26.74	26.76	26.77	26.78	26.79	26.81
2.34	26.82	26.83	26.84	26.86	26.87	26.88	26.89	26.90	26.92	26.93
2.35	26.94	26.95	26.96	26.98	26.99	27.00	27.01	27.02	27.04	27.05
2.36	27.06	27.07	27.08	27.10	27.11	27.12	27.13	27.14	27.16	27.17
2.37	27.18	27.19	27.20	27.21	27.22	27.24	27.25	27.26	27.27	27.28
2.38	27.29	27.31	27.32	27.33	27.34	27.35	27.36	27.37	27.39	27.40
2.39	27.41	27.42	27.43	27.45	27.46	27.47	27.48	27.49	27.51	27.52
2.40	27.53	27.54	27.55	27.56	27.57	27.58	27.60	27.61	27.62	27.63
2.41	27.64	27.65	27.66	27.67	27.68	27.69	27.71	27.72	27.73	27.74
2.42	27.75	27.76	27.77	27.79	27.80	27.81	27.82	27.83	27.84	27.85
2.43	27.86	27.87	27.88	27.90	27.91	27.92	27.93	27.94	27.95	27.96
2.44	27.97	27.98	27.99	28.01	28.02	28.03	28.04	28.05	28.06	28.07

TABLE I. - Continued. TABULATION OF CORRECTED ENTHALPY DROP FOR VARIOUS VALUES OF PRESSURE RATIO (FOR  $\gamma = 1.4$ )

$\frac{p_0}{p_1}$ ↓	$\Delta h' / \theta_{cr}$									
	0	.001	.002	.003	.004	.005	.006	.007	.008	.009
2.45	28.08	28.10	28.11	28.12	28.13	28.14	28.15	28.16	28.17	28.18
2.46	28.19	28.21	28.22	28.23	28.24	28.25	28.26	28.27	28.28	28.29
2.47	28.30	28.32	28.33	28.34	28.35	28.36	28.37	28.38	28.39	28.40
2.48	28.41	28.43	28.44	28.45	28.46	28.47	28.48	28.49	28.50	28.51
2.49	28.52	28.54	28.55	28.56	28.57	28.58	28.59	28.60	28.61	28.62
2.50	28.63	28.65	28.66	28.67	28.68	28.69	28.70	28.71	28.72	28.73
2.51	28.74	28.75	28.76	28.77	28.79	28.80	28.81	28.82	28.83	28.84
2.52	28.85	28.86	28.87	28.88	28.90	28.91	28.92	28.93	28.94	28.95
2.53	28.96	28.97	28.98	28.99	29.00	29.02	29.03	29.04	29.05	29.06
2.54	29.07	29.08	29.09	29.10	29.11	29.12	29.14	29.15	29.16	29.17
2.55	29.18	29.19	29.20	29.21	29.22	29.23	29.25	29.26	29.27	29.28
2.56	29.29	29.30	29.31	29.32	29.33	29.34	29.35	29.36	29.37	29.38
2.57	29.39	29.41	29.42	29.43	29.44	29.45	29.46	29.47	29.48	29.49
2.58	29.50	29.51	29.52	29.53	29.54	29.55	29.56	29.57	29.58	29.59
2.59	29.60	29.61	29.62	29.63	29.64	29.66	29.67	29.68	29.69	29.70
2.60	29.71	29.72	29.73	29.74	29.75	29.76	29.77	29.78	29.79	29.80
2.61	29.81	29.82	29.83	29.84	29.85	29.86	29.88	29.89	29.90	29.91
2.62	29.92	29.93	29.94	29.95	29.96	29.97	29.98	29.99	30.00	30.01
2.63	30.02	30.03	30.04	30.05	30.06	30.07	30.08	30.09	30.10	30.11
2.64	30.12	30.13	30.14	30.15	30.16	30.17	30.18	30.19	30.20	30.21
2.65	30.22	30.23	30.24	30.25	30.26	30.27	30.28	30.29	30.30	30.31
2.66	30.32	30.33	30.34	30.35	30.36	30.37	30.38	30.39	30.41	30.42
2.67	30.43	30.44	30.45	30.46	30.47	30.48	30.49	30.50	30.51	30.52
2.68	30.53	30.54	30.55	30.56	30.57	30.58	30.59	30.60	30.61	30.62
2.69	30.63	30.64	30.65	30.66	30.67	30.68	30.69	30.70	30.71	30.72
2.70	30.73	30.74	30.75	30.76	30.77	30.78	30.79	30.80	30.81	30.82
2.71	30.83	30.84	30.85	30.86	30.87	30.88	30.89	30.90	30.91	30.92
2.72	30.93	30.94	30.95	30.96	30.97	30.98	30.99	31.00	31.01	31.02
2.73	31.03	31.04	31.05	31.06	31.07	31.08	31.08	31.09	31.10	31.11
2.74	31.12	31.13	31.14	31.15	31.16	31.17	31.18	31.19	31.20	31.21
2.75	31.22	31.23	31.24	31.25	31.26	31.27	31.28	31.29	31.30	31.31
2.76	31.32	31.33	31.34	31.35	31.36	31.37	31.38	31.39	31.40	31.41
2.77	31.42	31.43	31.44	31.45	31.46	31.46	31.47	31.48	31.49	31.50
2.78	31.51	31.52	31.53	31.54	31.55	31.56	31.57	31.58	31.59	31.60
2.79	31.61	31.62	31.63	31.64	31.65	31.66	31.66	31.67	31.68	31.69
2.80	31.70	31.71	31.72	31.73	31.74	31.74	31.75	31.76	31.77	31.78
2.81	31.79	31.80	31.81	31.82	31.83	31.84	31.85	31.86	31.87	31.88
2.82	31.89	31.90	31.91	31.92	31.93	31.94	31.94	31.95	31.96	31.97
2.83	31.98	31.99	32.00	32.01	32.02	32.03	32.04	32.05	32.06	32.07
2.84	32.07	32.08	32.09	32.10	32.11	32.12	32.13	32.14	32.15	32.16

TABLE I. - Concluded. TABULATION OF CORRECTED ENTHALPY DROP FOR VARIOUS  
VALUES OF PRESSURE RATIO (FOR  $\gamma = 1.4$ )

$\frac{p_0}{p_6}$ ↓	$\Delta h' / \theta_{cr}$									
	0	.001	.002	.003	.004	.005	.006	.007	.008	.009
2.85	32.17	32.18	32.19	32.20	32.21	32.22	32.22	32.23	32.24	32.25
2.86	32.26	32.27	32.28	32.29	32.30	32.30	32.31	32.32	32.33	32.34
2.87	32.35	32.36	32.37	32.38	32.39	32.40	32.40	32.41	32.42	32.43
2.88	32.44	32.45	32.46	32.47	32.48	32.48	32.49	32.50	32.51	32.52
2.89	32.53	32.54	32.55	32.56	32.57	32.58	32.59	32.60	32.61	32.62
2.90	32.62	32.63	32.64	32.65	32.66	32.67	32.68	32.69	32.70	32.71
2.91	32.72	32.73	32.74	32.75	32.76	32.77	32.78	32.78	32.79	32.80
2.92	32.81	32.82	32.83	32.84	32.85	32.86	32.87	32.88	32.88	32.89
2.93	32.90	32.91	32.92	32.93	32.94	32.95	32.96	32.97	32.98	32.99
2.94	33.00	33.01	33.02	33.03	33.04	33.04	33.05	33.06	33.07	33.08
2.95	33.09	33.10	33.11	33.11	33.12	33.13	33.14	33.15	33.15	33.16
2.96	33.17	33.18	33.19	33.20	33.21	33.22	33.22	33.23	33.24	33.25
2.97	33.26	33.27	33.28	33.29	33.30	33.31	33.32	33.32	33.33	33.34
2.98	33.35	33.36	33.37	33.38	33.39	33.39	33.40	33.41	33.42	33.43
2.99	33.44	33.45	33.46	33.47	33.48	33.48	33.49	33.50	33.51	33.52
3.00	33.53	33.54	33.55	33.55	33.56	33.57	33.58	33.59	33.59	33.60
3.01	33.61	33.62	33.63	33.64	33.65	33.66	33.66	33.67	33.68	33.69
3.02	33.70	33.71	33.72	33.72	33.73	33.74	33.75	33.76	33.76	33.77
3.03	33.78	33.79	33.80	33.81	33.81	33.82	33.83	33.84	33.84	33.85
3.04	33.86	33.87	33.88	33.89	33.90	33.90	33.91	33.92	33.93	33.94

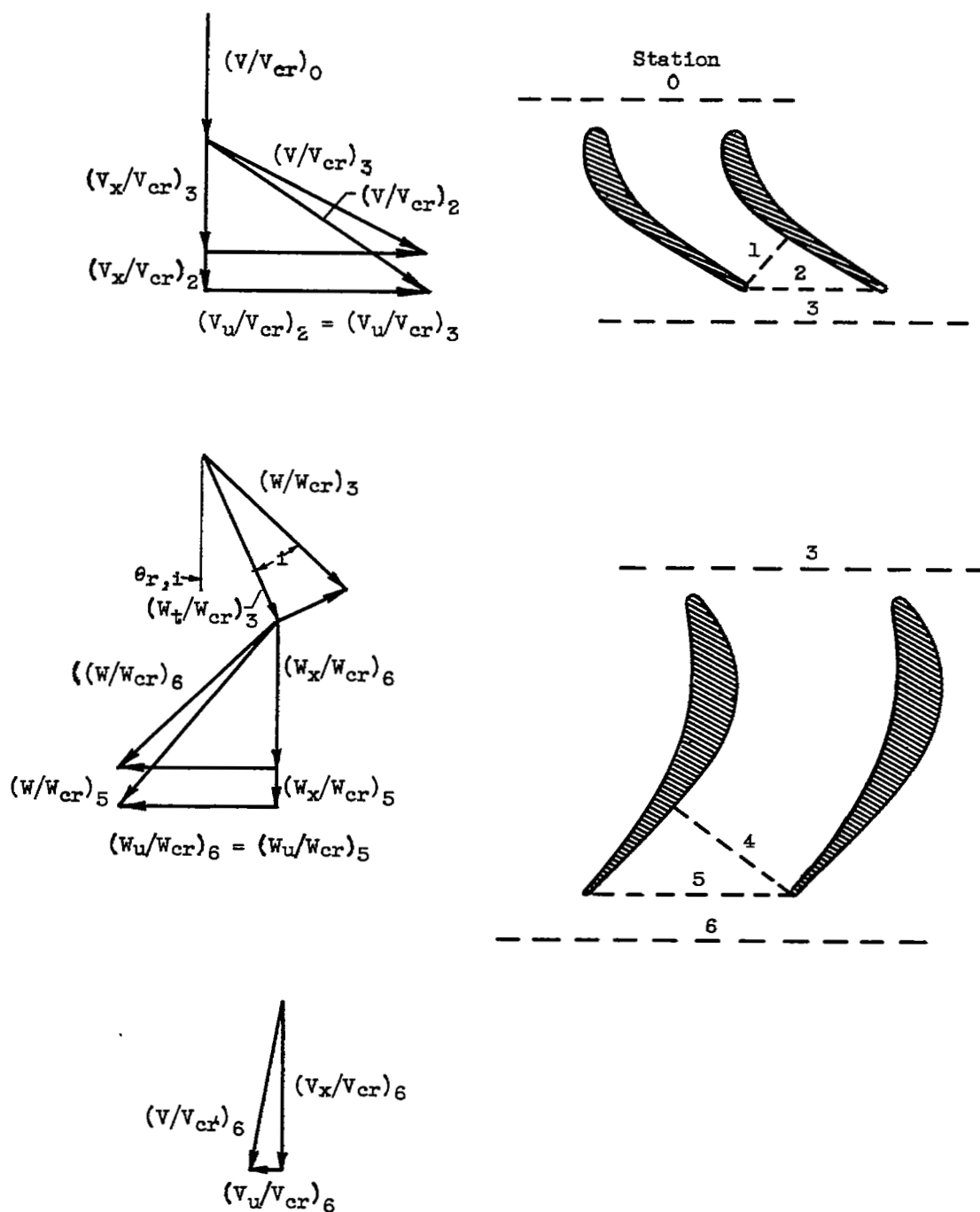


Figure 1. - Velocity diagrams and station designations used in turbine analysis.

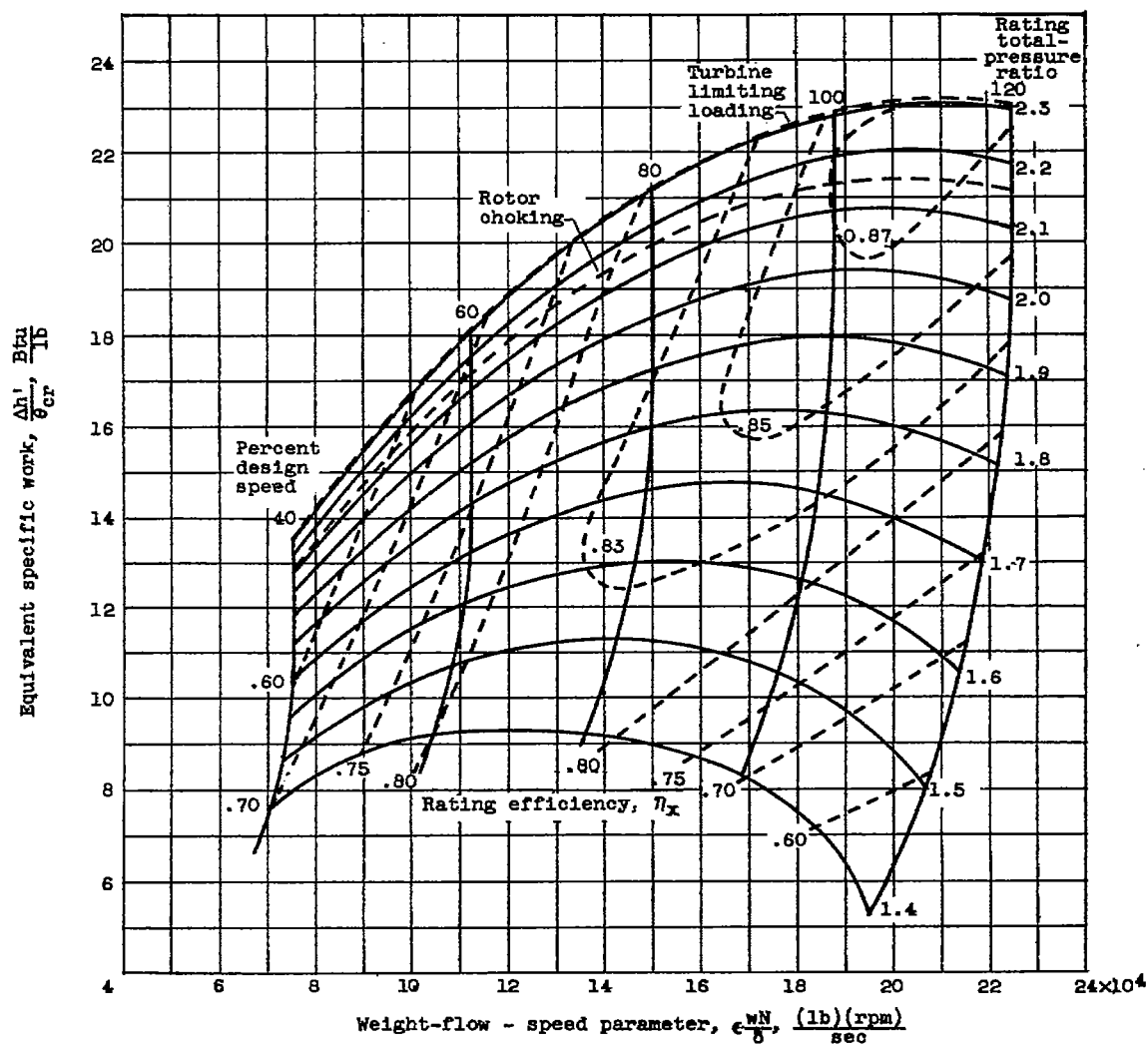


Figure 2. - Calculated performance map.

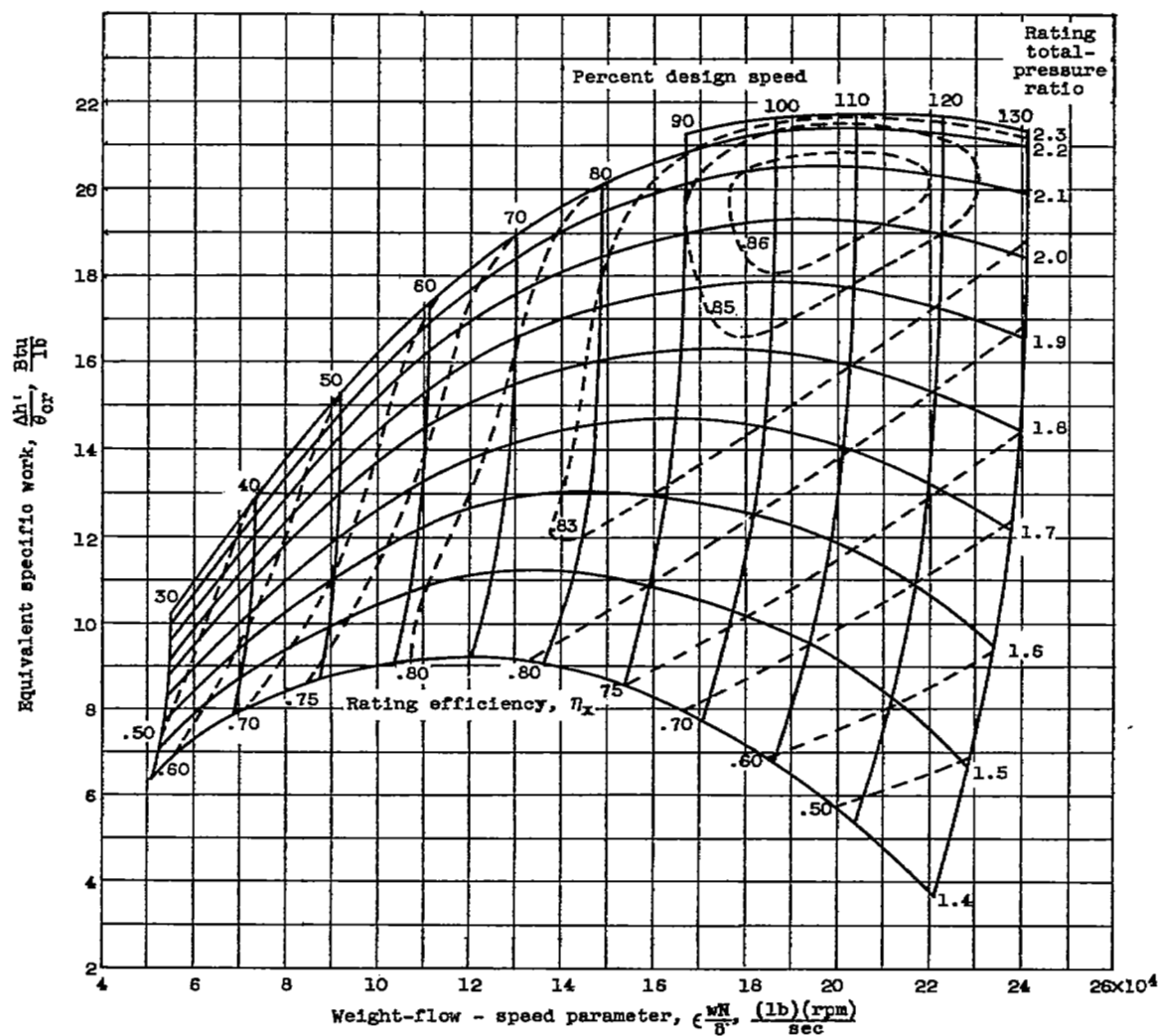
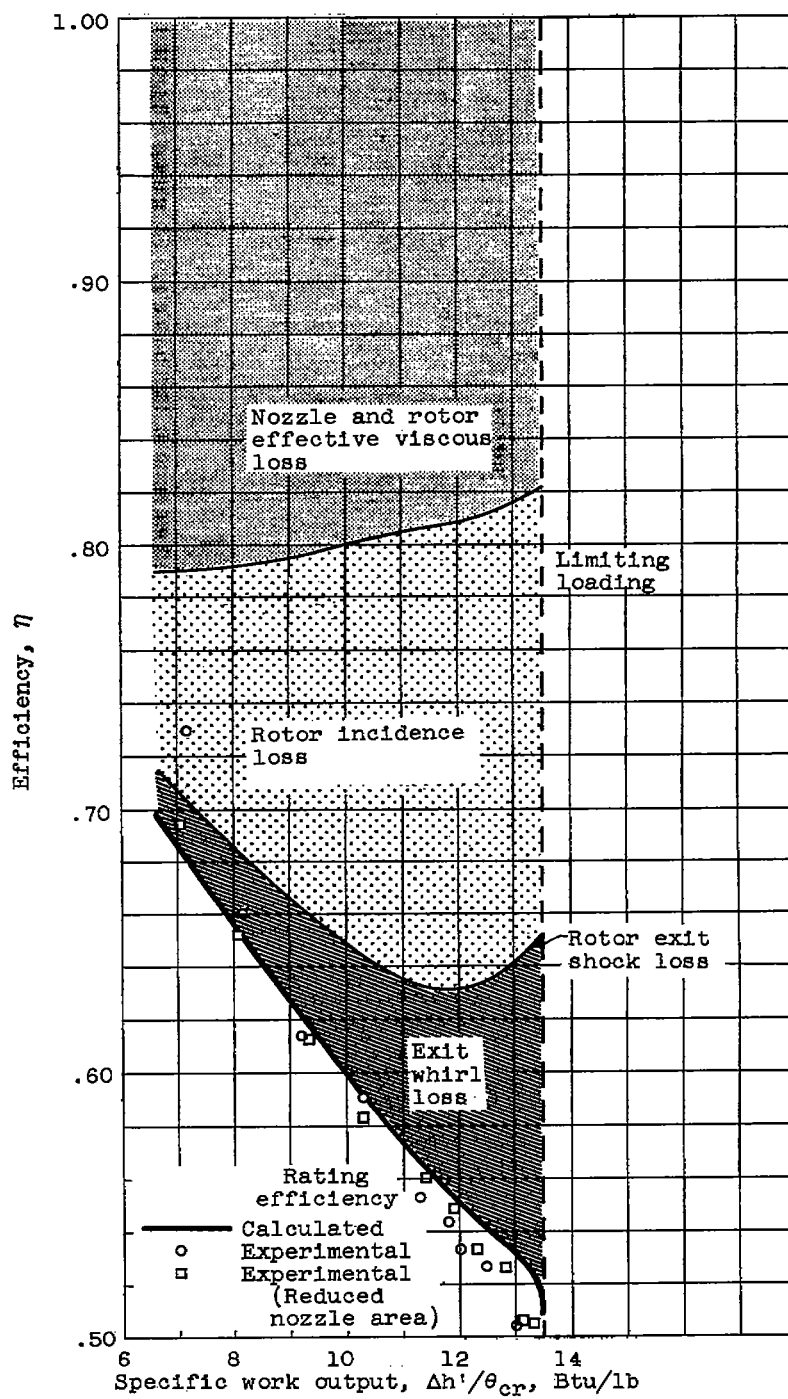
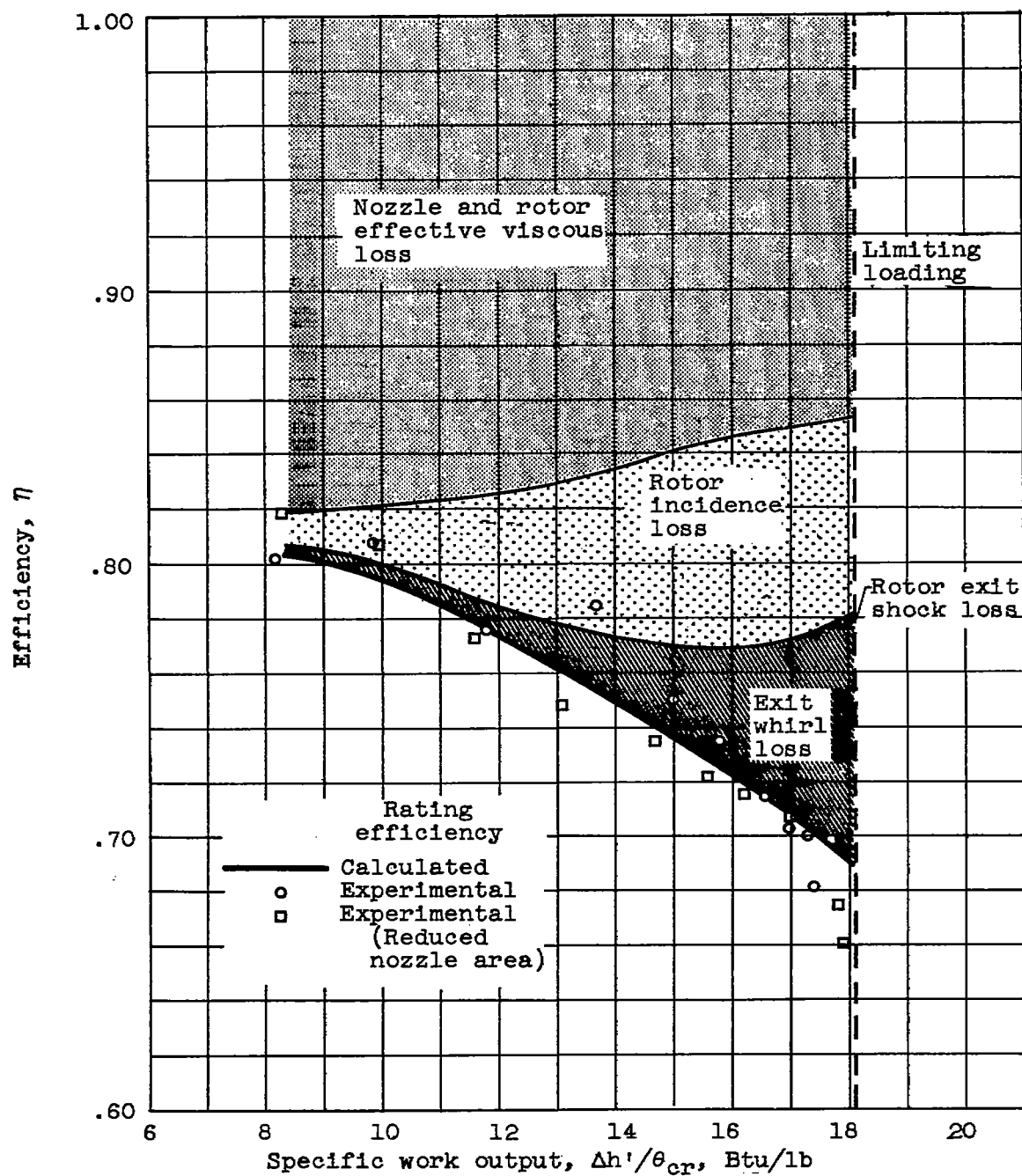


Figure 3. - Experimental performance of turbine (data from ref. 1).



(a) 40 Percent design speed.

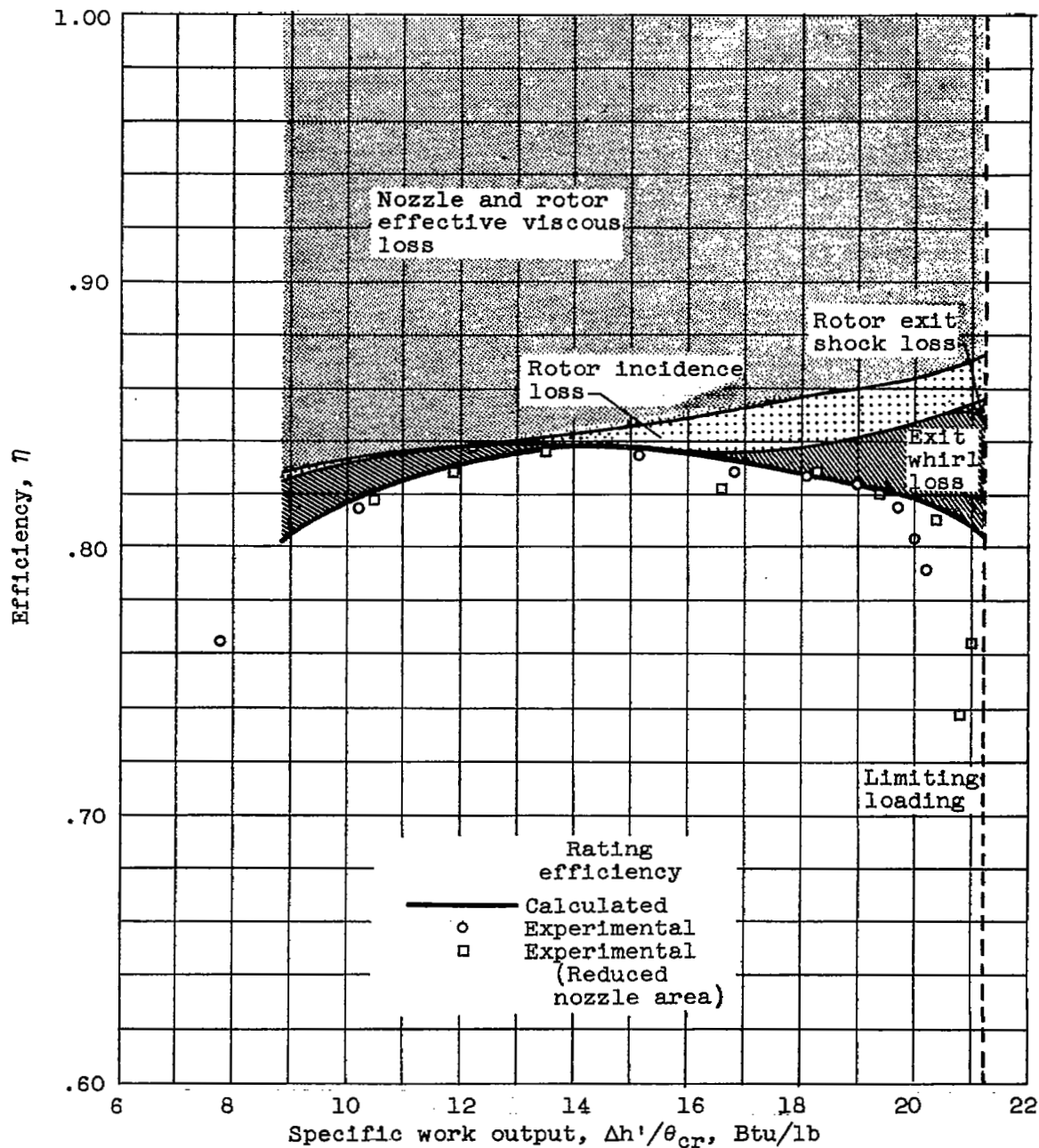
Figure 4. - Effect of various losses on efficiency.



(b) 60 Percent design speed.

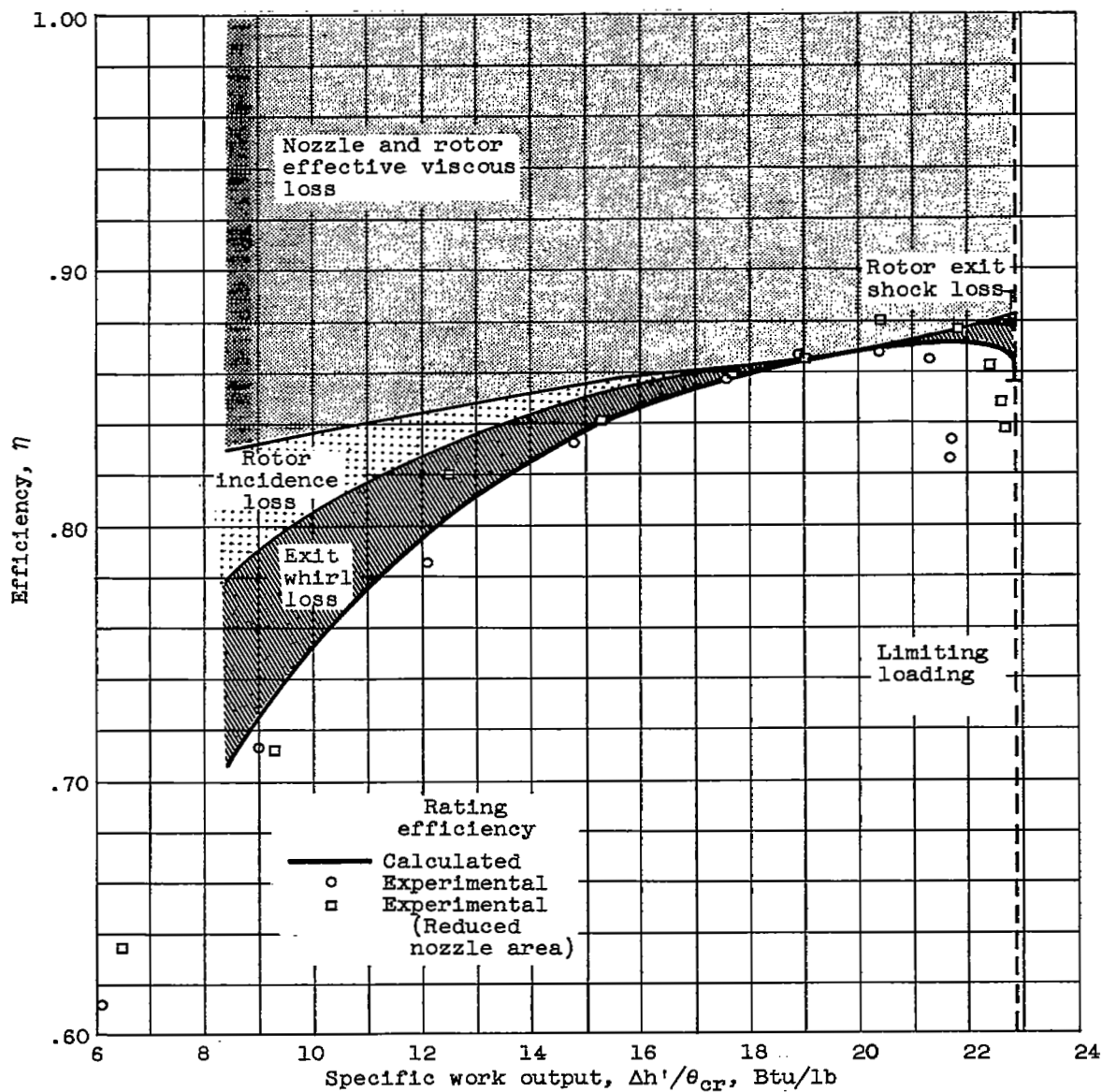
Figure 4. - Continued. Effect of various losses on efficiency.





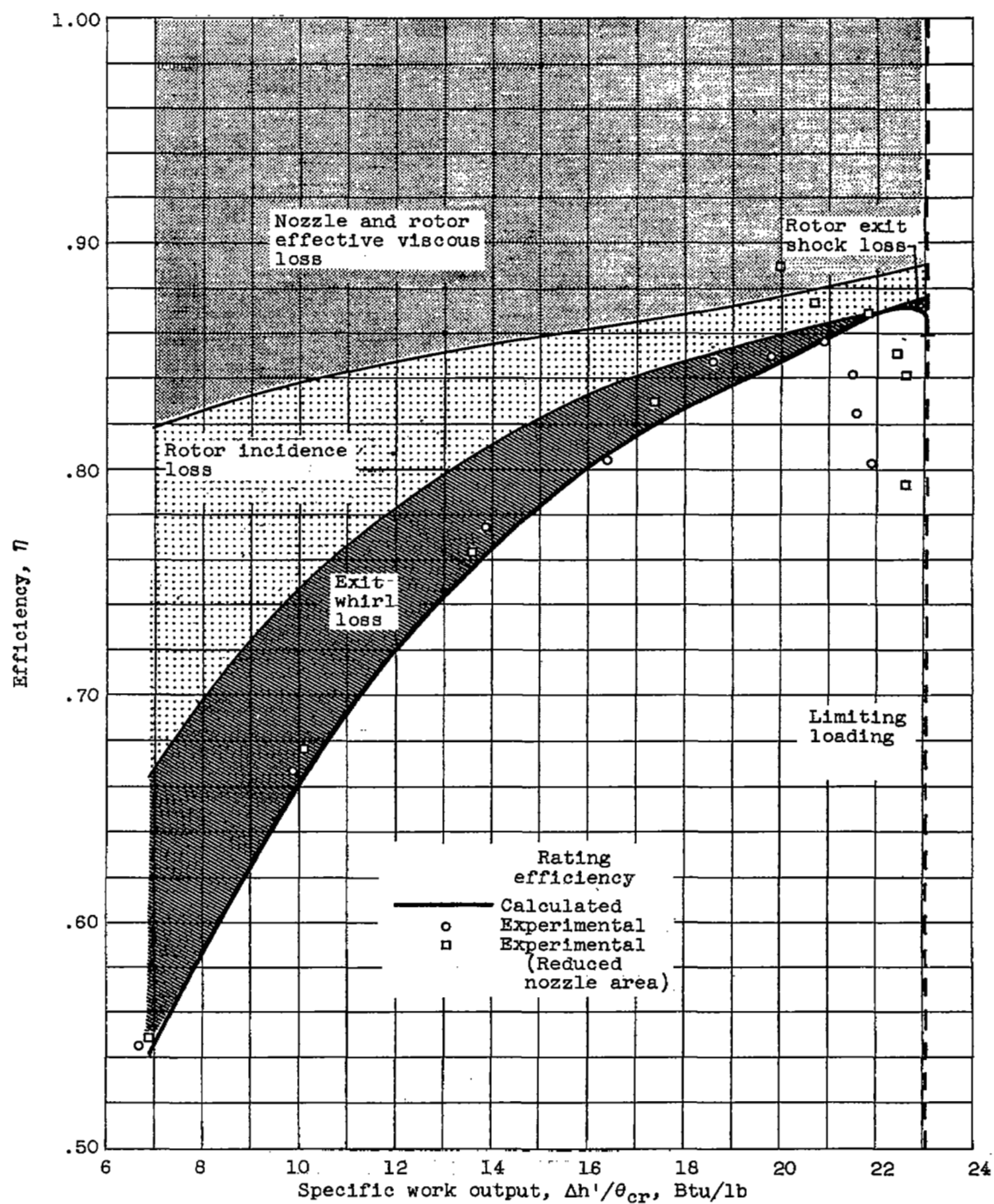
(c) 80 Percent design speed.

Figure 4. - Continued. Effect of various losses on efficiency.



(d) 100 Percent design speed.

Figure 4. - Continued. Effect of various losses on efficiency.



(e) 120 Percent design speed.

Figure 4. - Concluded. Effect of various losses on efficiency.

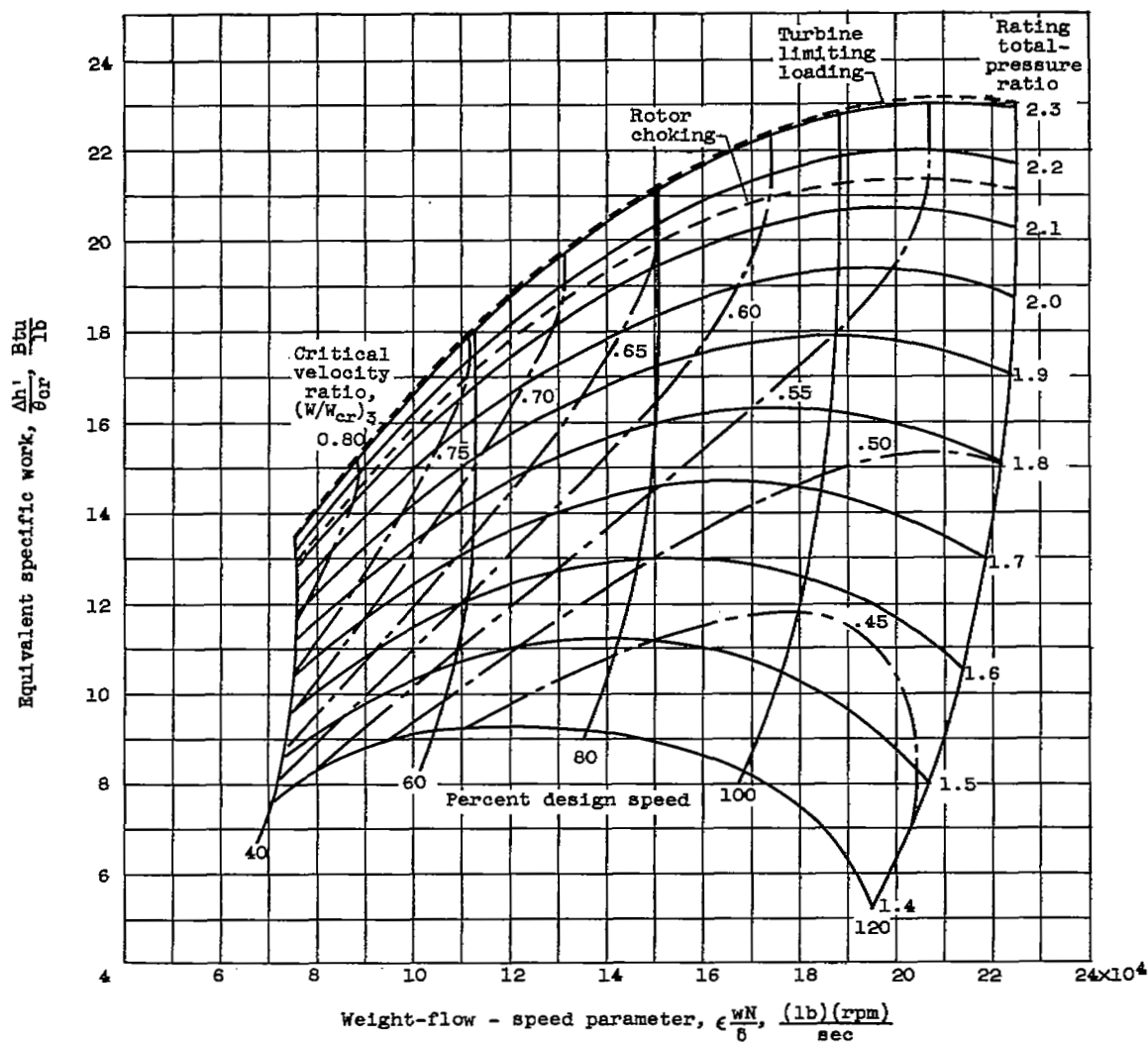


Figure 5. - Performance map showing variation in calculated rotor entrance critical velocity ratio at mean section.

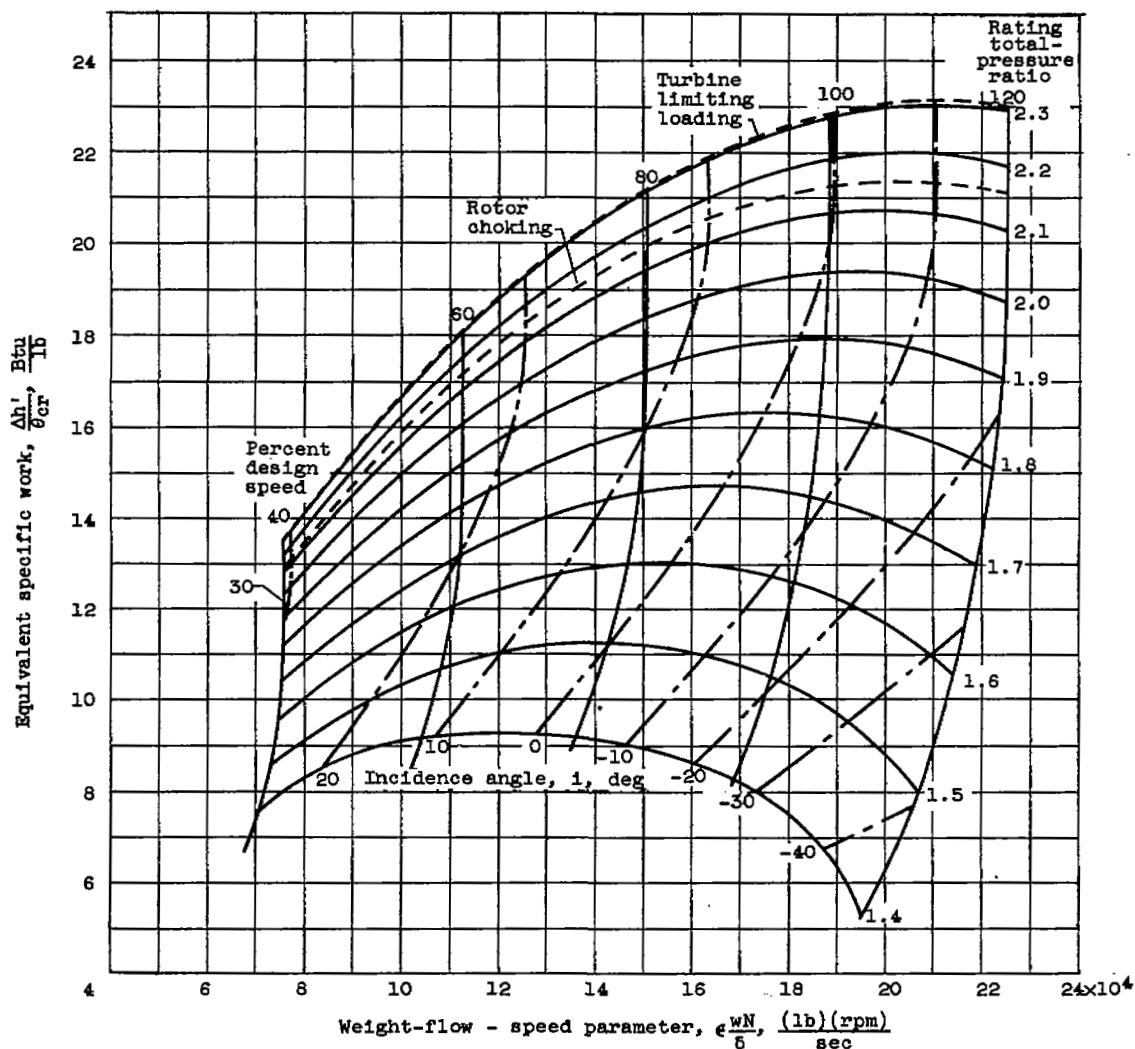
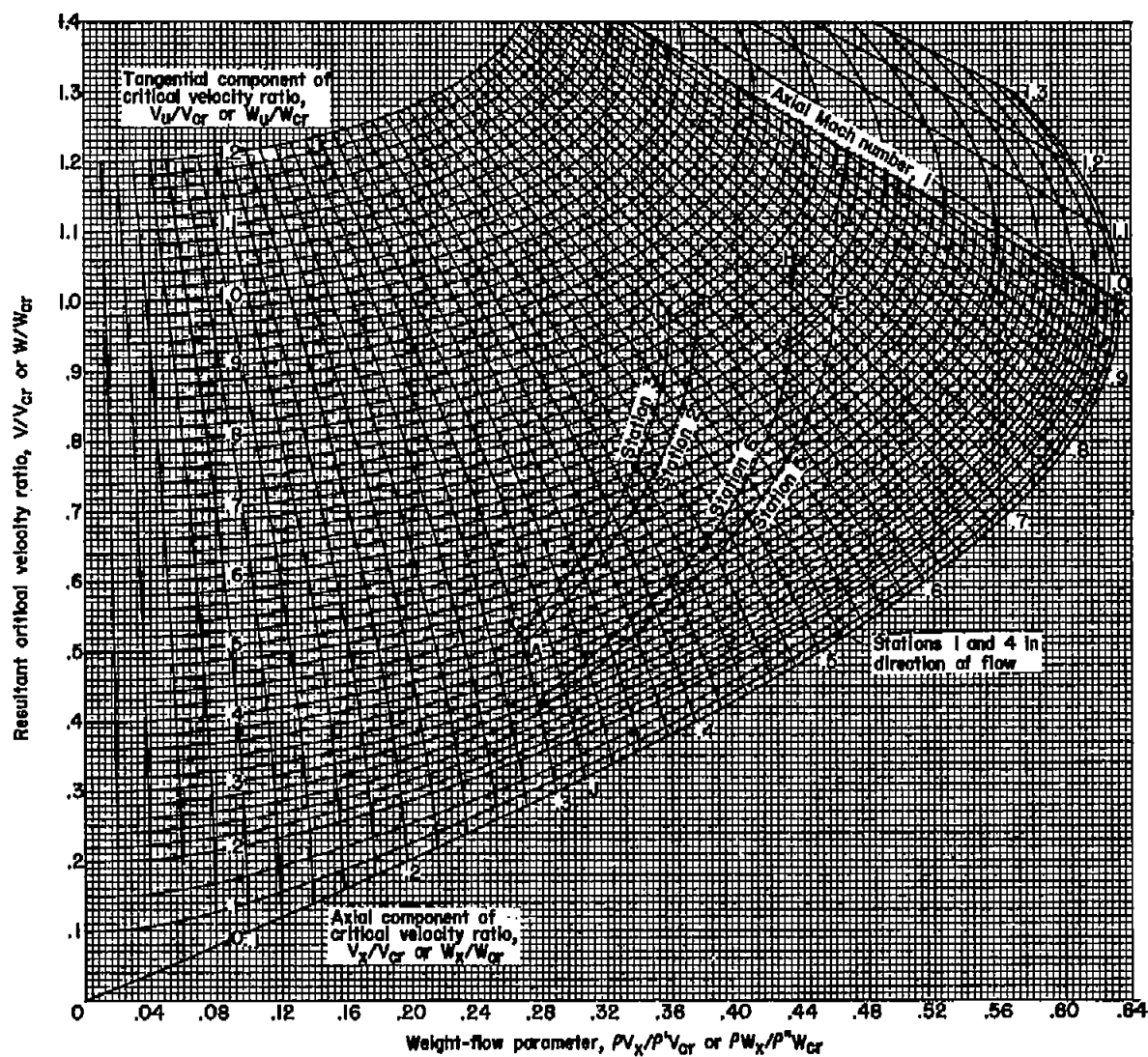


Figure 6. - Performance map showing variation in rotor incidence angle at mean section.

Figure 7.- Flow chart showing nozzle and rotor working curves.  $\gamma=1.4$ .

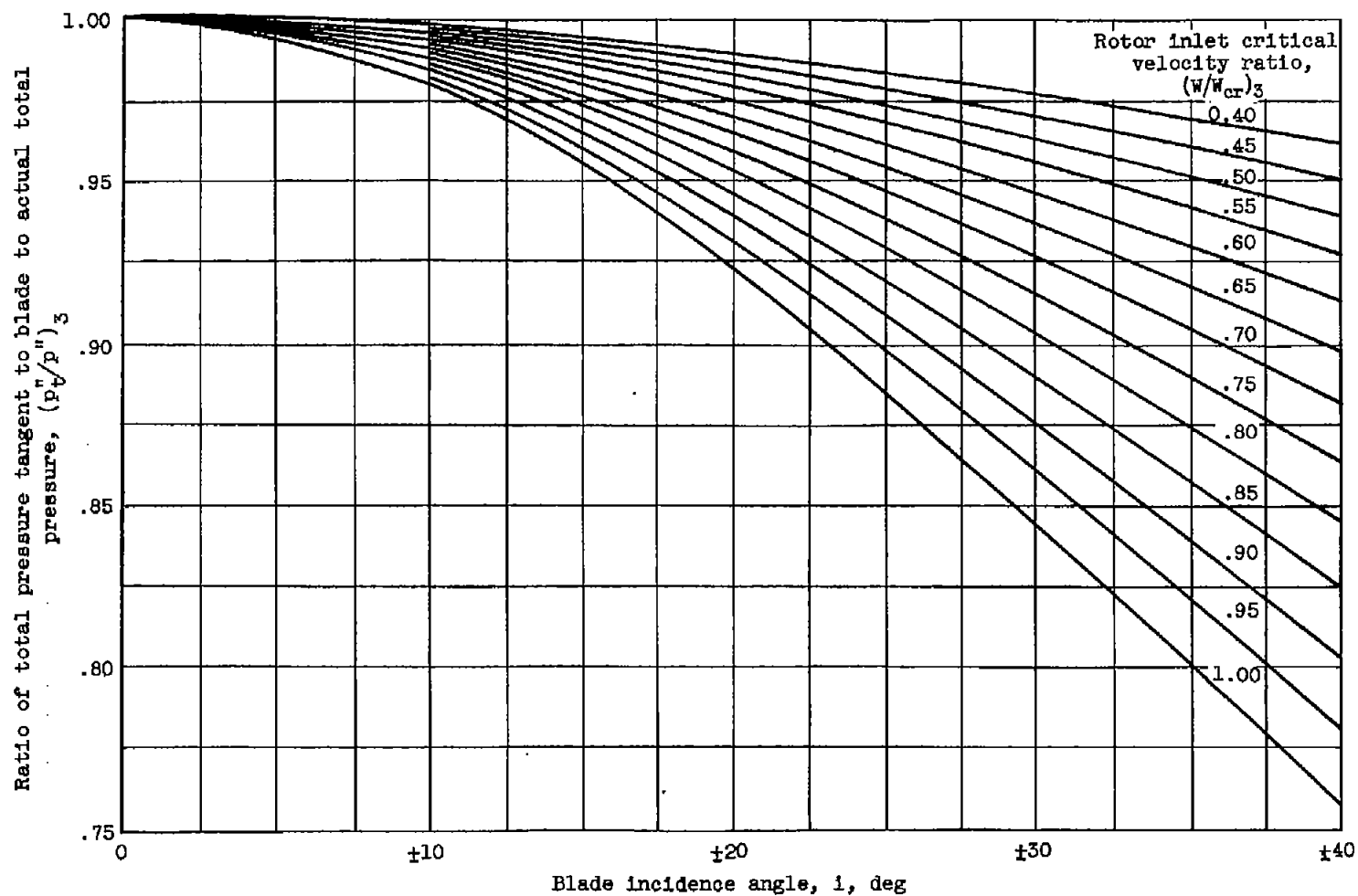


Figure 8. - Variation on total-pressure loss with blade incidence angle. Rotor inlet critical velocity ratio shown as parameter.

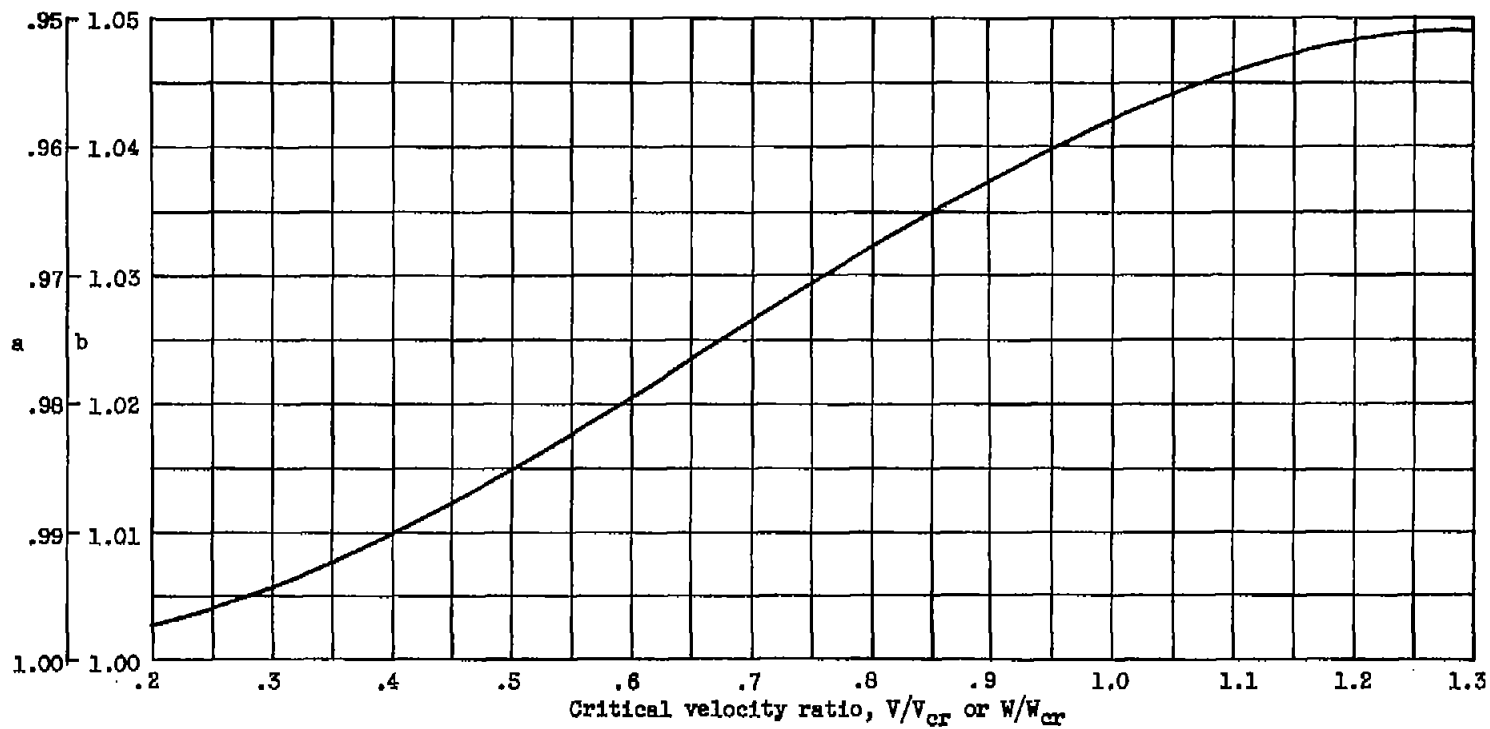


Figure 9. - Variation of loss parameters  $a$  and  $b$  with critical velocity ratio.



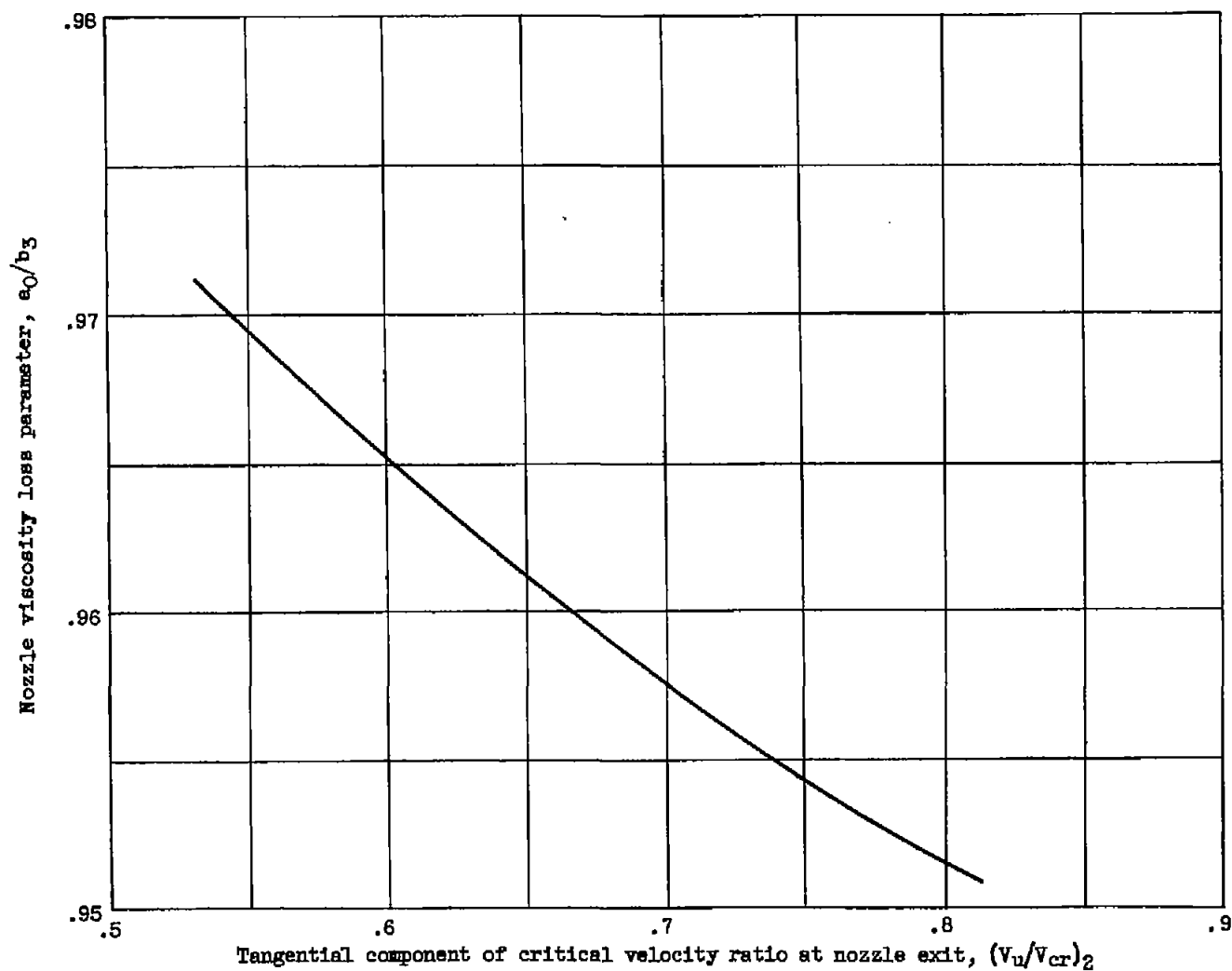


Figure 10. - Variation of nozzle viscosity loss parameter with tangential component of critical velocity ratio for turbine analyzed.

NASA Technical Library



3 1176 01437 6025

